Supporting Information

Photochemical Dimerization of Plakinidine B Leads to Potent Inhibition of the E3 Ubiquitin-protein Ligase CBL-B

Quan T. Khong,[a] Donghao Li,[b] Brice A. P. Wilson,[a] Kalina Ranguelova,[c] Masoumeh Dalilian,[a,d] Emily A. Smith,[a,d] Antony Wamiru,[a,d] Ekaterina I. Goncharova,[a,e] Tanja Grkovic,[a,f] Donna Voeller,[g] Stanley Lipkowitz,[g] Martin J. Schnermann,[b] Barry R. O'Keefe,*[,a,f] and Lin Du*[,a]

[a] Molecular Targets Program, Center for Cancer Research, National Cancer Institute, Frederick, Maryland 21702-1201, United States

[b] Chemical Biology Laboratory, Center for Cancer Research, National Cancer Institute, Frederick, Maryland 20850, United States

[c] Bruker BioSpin Corp, Billerica, MA 01821, United States

[d] Basic Science Program, Leidos Biomedical Research, Inc., Frederick National Laboratory for Cancer Research, Frederick, Maryland 21702-1201, United States

[e] Advanced Biomedical Computational Science, Frederick National Laboratory for Cancer Research, Frederick, MD 21702-1201, United States

[f] Natural Products Branch, Developmental Therapeutics Program, Division of Cancer Treatment and Diagnosis, National Cancer Institute, Frederick, Maryland 21701-1201, United States

[g] Women's Malignancies Branch, Center for Cancer Research, National Cancer Institute, National Institutes of Health, Bethesda, Maryland 20892-1578, United States

Table of Contents

Experimental Procedures

General Procedures

Optical rotations were recorded on a Rudolph Research Analytical Autopol IV polarimeter using a 0.25 dm cell in the solvent indicated. ECD spectra were collected with a Jasco J-1500 CD Spectrophotometer. UV data were measured with a Varian Cary® 50 UV-Vis Spectrophotometer. Absorbance spectra were obtained on a Jasco V-770 spectrophotometer operated by SpectraManager software. Fluorescence spectra were recorded on a PTI QuantaMaster steady-state spectrofluorometer operated by FelixGX4.2.2 software, with 5 nm excitation and emission slit widths, and a 0.1 s integration time. IR spectrum was recorded with a Bruker ALPHA II FT-IR spectrometer. NMR data were obtained on a Bruker Avance III NMR spectrometer equipped with a 3 mm cryogenic probe (600 MHz for ^{1}H, 150 MHz for ^{13}C). Structural assignments were made with additional information from gCOSY, gHSQC, and gHMBC experiments. HRESIMS data were collected on an Agilent Technology 6530 Accurate-mass Q-TOF LC/MS. X-band EPR measurements were performed on a bench-top Magnettech ESR5000 spectrometer manufactured by Freiberg Instruments for Bruker. HPLC separations were performed using a Varian ProStar 218 solvent delivery module equipped with a Varian ProStar 325 UV-Vis detector. All solvents were of LC-MS grade or better.

Animal Material

Specimens of the sponge *Plakortis* sp. were collected in Tonga in November 1997, and kept frozen until extraction. The collection was carried out by the Coral Reef Research Foundation under contract with the Natural Products Branch, U.S. National Cancer Institute, and taxonomically identified by Michelle Kelley. A voucher specimen (voucher ID # 0CDN5480) was deposited at

the Smithsonian Institution, Washington, D.C. The animal material (205 g, wet weight) was ground and processed using the standard NCI method[1] for marine samples to provide 19.9 g of organic extract (NSC # C17897).

1. McCloud, T. G., High throughput extraction of plant, marine and fungal specimens for preservation of biologically active molecules. *Molecules* **2010**, *15*, 4526-4563.

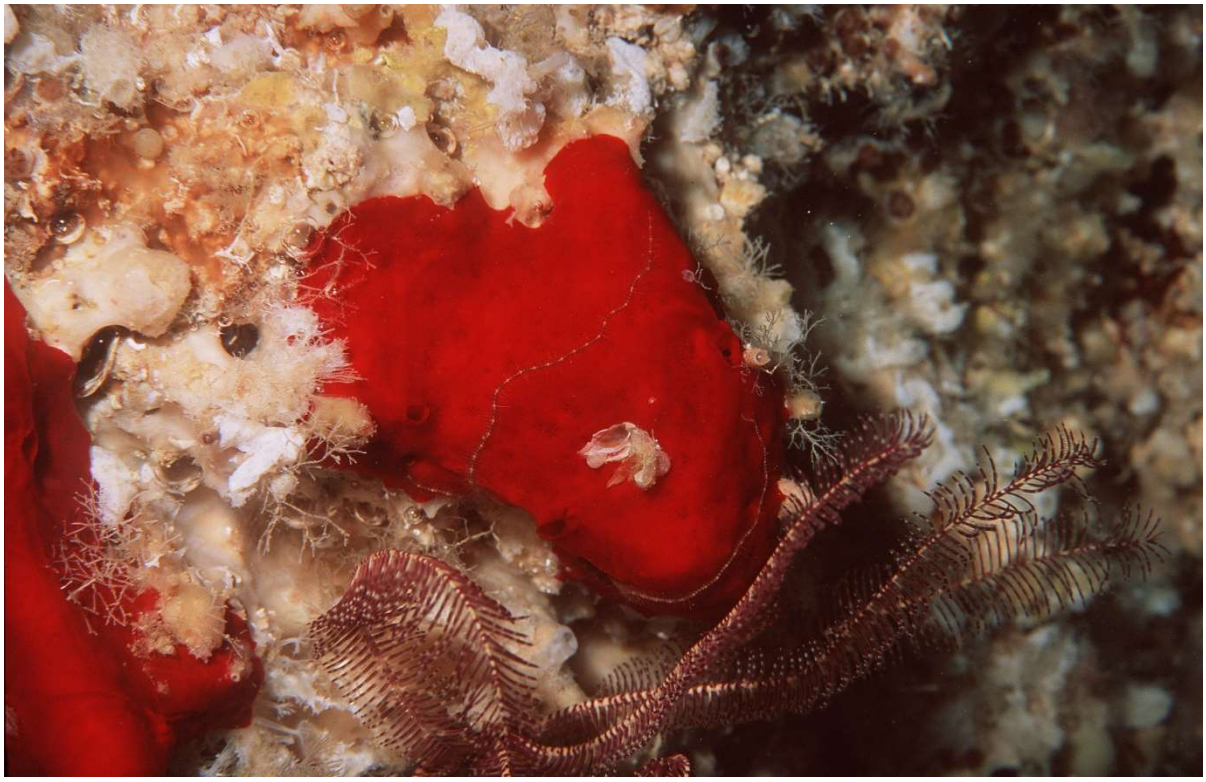

In situ photograph of the sponge *Plakortis* sp.

Purification of Compound (±)**-1**

The organic crude extract (NSC # C017897, 1 g) was subjected to a C8 solid-phase extraction (SPE) process (250 mg extract loading on each 2 g C8 SPE cartridge eluted with gradients of 5%, 20%, 40%, 60%, 80%, and 100% MeOH in H_2O and 50% MeOH in MeCN) to generate seven

fractions. The active fractions Fr. 1-5 (combined mass 208 mg) was further separated by prep-HPLC using a Kinetex 5 μm EVO C18 column (110 Å, 250 × 21.2 mm) with flow rate of 10 mL/min (eluted with 10% – 100% MeCN with 0.1% TFA) to give 15 fractions. The subfraction 5 (RT = 20.01 min) was determined to be the known compound plakinidine B (**2**, 5.8 mg). Further purification of the subfraction 12 (RT = 31.05 min) by semi-prep HPLC using a Kinetex 5 μm F5 column (110 Å, 250 × 10 mm) with flow rate of 4 mL/min (eluted with 25% MeCN with 0.1% TFA) yielded the racemic plakoramine A [(±)-**1**, 0.9 mg] (RT = 10.72 min). Chiral-phase HPLC separation of (±)-**1** on a Lux 5 μm i-Amylose-3 column (1000 Å, 250 × 4.6 mm) with flow rate of 1 mL/min (eluted with 40% MeCN with 0.1% TFA) led to the purified enantiomers (+)-plakoramine A [(+)-**1**, 0.25 mg] (RT = 5.82 min) and [(-)-plakoramine A [(-)-**1**, 0.25 mg] (RT = 9.47 min).

2. Thornburg, C. C.; Britt, J. R.; Evans, J. R.; Akee, R. K.; Whitt, J. A.; Trinh, S. K.; Harris, M. J.; Thompson, J. R.; Ewing, T. L.; Shipley, S. M.; Grothaus, P. G.; Newman, D. J.; Schneider, J. P.; Grkovic, T.; O'Keefe, B. R. NCI Program for Natural Product Discovery: A Publicly-Accessible Library of Natural Product Fractions for High-Throughput Screening. *ACS Chem. Biol.* **2018**, *13*, 2484-2497.

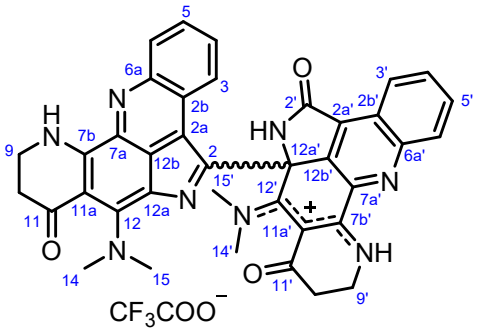

plakoramine A [(±)-**1**]

Plakoramine A [(±)-1]: red solid; UV (MeOH) λ_{max} (log ε) 245 (4.39), 283 (4.28), 346 (4.33), 346 (4.33), 544 (3.62); IR (neat) ν_{max} 3237, 2922, 2852, 1687, 1631, 1603, 1576, 1558, 1433, 1406,

1354, 1298, 1276, 1256, 1195, 1135, 1091, 1076, 1061, 1033, 800, 722, 571, 535 cm^{-1}; ^{1}H and ^{13}C NMR data, see Table S1; HRESIMS *m/z* 647.2510, $[M]^+$ (calcd for $C_{38}H_{31}N_8O_3^+$, 647.2514); **(+)-1**: $[\alpha]^{20}_D$ 340 (c 0.04, MeOH); CD (MeOH) λ_{max} ($\Delta\varepsilon$) 230 (-13.9), 263 (-10.2), 352 (16.4), 421 (-2.8), 555 (1.2); **(-)-1**: $[\alpha]^{20}_D$ -335 (c 0.04, MeOH); CD (MeOH) λ_{max} ($\Delta\varepsilon$) 230 (12.6), 263 (8.9), 352 (-15.2), 421 (3.0), 555 (-0.7).

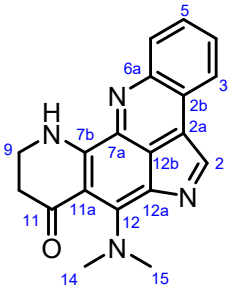

plakinidine B (**2**)

Plakinidine B (2): orange solid; ^{1}H NMR (DMSO-d_6, 600 MHz) δ_H 10.73 (1H, s, NH-8), 8.76 (1H, s, H-2), 8.51 (1H, dd, *J* = 8.0, 1.5, H-3), 8.25 (1H, dd, *J* = 8.0, 1.5, H-6), 7.87 (1H, m, H-4), 7.82 (1H, m, H-5), 3.83 (2H, td, *J* = 7.3, 3.5, H_2-9), 3.76 (3H, brs, H_3-15), 3.44 (3H, brs, H_3-14), 2.66 (2H, t, *J* = 7.3, H_2-10); ^{13}C NMR (DMSO-d_6, 150 MHz) δ_C 187.2 (C-11), 158.5 (C-7b), 153.1 (C-12), 143.8 (C-6a), 140.9 (C-7a), 130.9 (C-6), 130.2 (C-4), 128.4 (C-5), 126.2 (C-2), 124.3 (C-3), 123.5 (C-2b), 121.7 (C-2a), 120.2 (C-12a), 115.3 (C-12b), 103.5 (C-11a), 49.1 (C-14), 44.3 (C-15), 38.8 (C-9), 36.7 (C-10); HRESIMS *m/z* 317.1405, $[M+H]^+$ (calcd for $C_{19}H_{17}N_4O^+$, 317.1397).

Computational Details

Conformational analyses were carried out using ComputeVOA v1.1. Geometry, frequency, and ECD calculations were applied at the DFT (density functional theory) and TD-DFT (time-dependent density functional theory) levels [B3LYP functional/DGDZVP basis set] with Gaussian' 16 carried out in MeOH phase using the COSMO solvation model. The low energy conformers

were selected from those with energies predicted to be within 2.0 kcal/mol of the lowest-energy conformer. The calculated ECD spectra of these conformers were summed after a Boltzmann statistical weighting and adjusted by applying a sigma value of 0.2 eV prior to the comparison with the experimentally obtained ECD data.

CBL-B Biochemical Assay

Chromatography fractions and pure compounds were evaluated for activity in a CBL-B biochemical assay as previously described.[3] In brief, dose response experiments with the purified compounds were carried out in Tris− HCl buffer (pH 7.5) that contained 15 nM E1 protein (UBE1), 75 nM E2 protein (Ube2d2), 112 nM CBL-B protein (N1/2 Construct), 75 nM biotinylated ubiquitin, 750 nM ubiquitin, 0.1 mM dithiothreitol, 0.5 mg/mL bovine gelatin type B, 0.5 mM magnesium chloride, and 0.01% Triton X-100. Addition of ATP into the enzyme solution initiated the enzymatic reaction cascade. Initiated reactions were then transferred to plates that had been precoated overnight with 10 μg/mL polyubiquitin binding portion of CBL-B (UBA) which allowed for the binding and specific enrichment of autopolyubiquitinated CBL-B. After 1 h, the reactions were quenched, and the reaction plates were sealed and incubated overnight at room temperature. The following day, reaction plates were probed with avidin-conjugated horse radish peroxidase and washed three times; then, an avidin-HRP dependent fluorescent signal (indicating the presence of avidin-HRP/biotin-polyubiquitin complexes bound by the UBA coated plate) was detected (excitation 325 nm, emission 420 nm) using a Tecan Infinite M1000 plate reader.

3. Wilson, B. A. P.; Voeller, D.; Smith, E. A.; Wamiru, A.; Goncharova, E. I.; Liu, G.; Lipkowitz, S.; O'Keefe, B. R. *SLAS Discovery* **2021**, 1.

Quantification of Plakoramine A [(±)-1]

Standard curve. A stock solution of [(±)-**1**] in MeOH (0.3 mg/mL) was serially diluted by 2, 4, 8, 16, 32, 64, and 128 folds and analyzed by HPLC-PDA (UV 254 nm) to obtain the standard quantification curve.

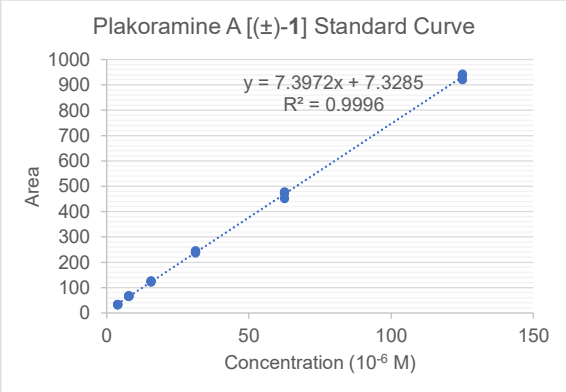

Time-dependent Production of (±)-1 by Irradiation of 2 with White Light

Ambient condition. 0.1 mg plakinidine B (**2**) was dissolved in 100 uL MeCN/H_2O (1/1) in a 4-mL scintillation vial (14.75 mm x 45 mm), capped, and irradiated under white light (15 W LED) at a 25 cm distance. The production of plakoramine A [(±)-**1**] was quantified at 30, 60, 120, 180, and 240 minutes. At each time point, 5 uL reaction solution was diluted by 25 ul MeOH prior to HPLC-PDA (254 nm) analysis. The (±)-**1** concentration was calculated as averages of three independent experiments ± SEM. The time-course graph was analyzed with Nonlinear Regression using Graphpad Prism 9.4.1 to generate the following fitting curve (red) with an equation.

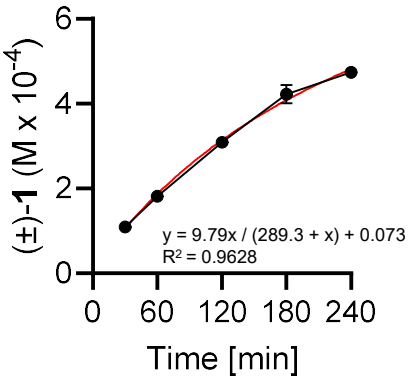

Partially De-Oxygenated Conditions. MeCN and H_2O were roughly degassed by purging the solvents with nitrogen flows for 30 minutes. 0.1 mg of plakinidine B (**2**) in a 4-mL scintillation vial was protected by nitrogen during sample preparation. Each 50 uL purged MeCN and H_2O was quickly transferred into the vial, capped, and irradiated under the white light (15 W LED) at a 25 cm distance. The production of plakoramine A [(±)-**1**] was quantified at 180 minute. The (±)-**1** concentration was calculated as averages of three independent experiments ± SEM.

- Light source: Ceiling LED tube light with plastic cover (Energy Focus® LEDFL T8-840-415-2B2F, 100-277 V, 50/60 Hz, 0.13 A, 15 W CCT 4000, 25 cm irradiation path)

ROS Studies

All reaction samples were diluted with MeOH (1 : 1) and directly subjected to LCMS analysis. All experiments were conducted in triplicate with a negative control (**2** + vehicle).

Hydrogen Peroxide. A 100 µM solution of **2** in 10 mM PBS (pH = 7.4) was generated from a 10 mM DMSO stock solution. A solution of hydrogen peroxide (100 mM in H_2O stock) was added such that the final concentration of H_2O_2 was 500 µM. The sample was incubated for 2 h at room temperature in the dark.

Fenton Conditions. A 100 µM solution of **2** in 50 mM $NaHPO_4$ (pH = 6.0) was generated from a 10 mM DMSO stock solution. Solutions of $FeCl_2$ tetrahydrate (50 mM H_2O stock) and hydrogen

peroxide (100 mM H_2O stock) were added in succession such that the final concentration of each was 500 μM, and the sample was incubated for 5 min at room temperature in the dark.

Thermal $^1O_2$ Generation. Naphthalene endoperoxide (**3**) was synthesized according to a known procedure (*J. Org. Chem.* **1989**, *54*, 726-728). A 20 mM solution of **3** in H_2O was prepared. A solution of 100 μM **2** and 4 mM naphthalene endoperoxide in 10 mM PBS was generated from their respective stock solutions. The sample was heated to 40 °C in a HPLC vial for 4 h in the dark.

Superoxide. A 100 μM solution of **2** in 1/1 MeCN/H_2O was generated from a 10 mM DMSO stock solution. A solution of KO_2 (5 mM in DMSO stock) was added such that the final concentration of KO_2 was 500 μM, and the sample was incubated for 2 h at room temperature in the dark.

Photooxidation of ABDA Sensitized by Plakinidine B (2)

Plakinidine B (**2**, 0.5 mg) was dissolved in 50 μL MeCN/H_2O (1/1) in a 20-mL scintillation vial. The solution was irradiated with white light (15 W LED) for 5 minutes prior to the addition of 1.5 mg of 9,10-anthracenediyl-bis(methylene)dimalonic acid (ABDA) which was dissolved in 20 μL DMSO. The mixture was diluted with 500 μL MeCN/H_2O (1/1) and irradiated under white light (15 W LED) for another 5 hours. The same reaction was carried out parallelly in 9 scintillation vials, respectively. The reaction mixtures were combined and dried under the nitrogen gas. The product mixture was re-dissolved in DMSO and subjected to prep-HPLC separation using a Kinetex 5 μm AXIA C18 column (110 Å, 250 × 21.2 mm) with a flow rate of 10 mL/min (eluted with 15% – 55% MeCN with 0.1% FA in 80 minutes) to yield **4** (1.3 mg, t_R = 22 min) and **5** (2.5 mg, t_R = 52 min).

Compound **5** gradually decomposed in acetone-d_6 and DMSO-d_6 during NMR measurement so only incomplete NMR data sets were obtained. The compound is relatively stable in methanol-d_4

enabling the collection of the long HMBC and ^{13}C NMR data. Interestingly, the resonances of H-12 and C-12 were not observed in the ^{1}H, ^{13}C, and HSQC NMR spectra measured in methanol-d_4, though the ^{13}C chemical shift of C-12 was interpreted based on the HMBC correlations from H_2-11 to C-12. In DMSO-d_6 and acetone-d_6, H-12 was well observed at δ_H 4.38 (1H, t, J = 9.9) and δ_H 4.35 (1H, t, J = 9.8), respectively. Similar to compound **5**, the ^{1}H resonance of H-12 was also not observed in the ^{1}H NMR spectrum of **4** that was measured in methanol-d_4. Compound **4** underwent decomposition in methanol-d_4 during the collection of the long ^{13}C NMR spectrum which prevented further attempts to detecting H-12 with other NMR solvents.

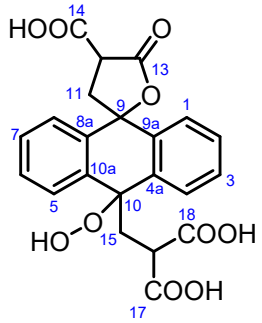

4

2-((4'-carboxy-10-hydroperoxy-5'-oxo-4',5'-dihydro-3'*H*,10*H*-spiro[anthracene-9,2'-furan]-10-yl)methyl)malonic acid (4): ^{1}H NMR (Methanol-d_4, 600 MHz) δ_H 7.88 (1H, d, J = 7.6), 7.85 (1H, d, J = 7.6) 7.61 (1H, d, J = 7.6), 7.36 (1H, d, J = 7.6) (H-1, H-4, H-5, and H-8), 7.47 (4H, m, H-2, H-3, H-6, H-7), 3.62 (1H, t, J = 6.2, H-16), 2.97 (1H, d, J = 13.3, H_2-11a), 2.85 (1H, d, J = 13.3, H_2-11b), 2.42 (2H, m, H_2-15); HRESIMS m/z 441.0830, $[M-H]^-$ (calcd for $C_{22}H_{17}O_{10}^-$, 441.0827).

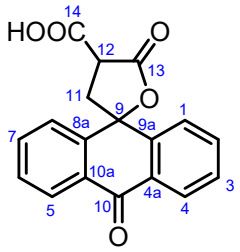

5

5',10-dioxo-4',5'-dihydro-3'*H*,10*H*-spiro[anthracene-9,2'-furan]-4'-carboxylic acid (5):

^{1}H NMR (Methanol-d_4, 600 MHz) δ_H 8.26 (1H, d, J = 7.8), 8.22 (1H, d, J = 7.8) (H-4 and H-5), 7.79 (2H, m, H-2, H-7), 7.77 (1H, m), 7.58 (1H, d, J = 8.0) (H-1 and H-8), 7.62 (2H, m, H-3, H-6), 2.94 (1H, d, J = 13.7, H_2-11a), 2.79 (1H, d, J = 13.7, H_2-11b); ^{13}C NMR (Methanol-d_4, 150 MHz) δ_C 184.1 (C-10), 174.8 (C-14), 170.8 (C-13), 146.0, 145.4 (C-8a and C-9a), 135.6 (C-7), 135.4 (C-2 and C-7), 131.1, 131.0 (C-4a and C-10a), 130.3, 130.2 (C-3 and C-6), 128.8, 128.2 (C-4 and C-5), 126.3, 125.4 (C-1 and C-8), 82.2 (C-9), 47.9 (C-12), 45.9 (C-11); ^{1}H NMR (acetone-d_6, 600 MHz) δ_H 8.26 (1H, d, J = 7.8), 8.22 (1H, d, J = 7.8) (H-4 and H-5), 7.84 (2H, m, H-2, H-7), 7.83 (1H, m), 7.66 (1H, m) (H-1 and H-8), 7.67 (2H, m, H-3 and H-6), 4.35 (1H, t, J = 9.8, H-12), 3.02 (1H, dd, J = 13.8, 9.8, H_2-11b), 2.95 (1H, dd, J = 13.8, 9.8, H_2-11a);

^{1}H NMR (DMSO-d_6, 600 MHz) δ_H 8.18 (1H, d, J = 7.8), 8.16 (1H, d, J = 7.8) (H-4 and H-5), 7.87 (1H, t, J = 7.8), 7.81 (1H, t, J = 7.8) (H-7 and H-2), 7.72 (1H, d, J = 7.8), 7.64 (1H, m) (H-1 and H-8), 7.66 (2H, m, H-3 and H-6), 4.38 (1H, t, J = 9.9, H-12), 2.85 (2H, m, H_2-11);

HRESIMS m/z 309.0756, $[M+H]^+$ (calcd for $C_{18}H_{13}O_5^+$, 309.0757).

Detection and Quantification of Singlet Oxygen by Electron Paramagnetic Resonance (EPR)

Plakinidine B (**2**) was dissolved in MeCN/H_2O (1/1) at 1 mg/mL. A specific spin trap 2,2,6,6-tetramethyl-4-piperidone (4-Oxo-TEMP) that selectively and rapidly forms a stable radical 4-Oxo-TEMPO with $^1O_2$ was added to the plakinidine B solution to a final concentration of 5 mM. The reaction between 4-Oxo-TEMP and singlet oxygen was monitored by EPR under white light

(Fluorescent tube light bulbs, 32 Watts, 4100 K color temperature, 2800 Lumens light output, The irradiation path is ~ 12 ft) exposure for 4 hours at room temperature. The singlet oxygen concentration was calculated based on the stable radical 4-Oxo-TEMPO concentration formed after 4-Oxo-TEMP oxidation by $^1O_2$.

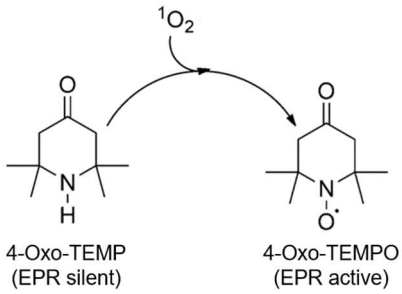

The EPR instrument operated at microwave frequency of 9.47 GHz at room temperature with the g-factor (g_e) of 2.0059 and the hyperfine splitting (a_N) of 1.6 mT for the detection of the 4-oxo-TEMPO signal. All measurements employed a center field of 337.2 mT, sweep width of 10 mT, microwave power of 10 mW, 0.1 mT modulation amplitude with 100 kHz modulation frequency, sweep time of 30 sec, number of scans – 4. Quantitative EPR analysis was performed using reference free SpinFit and SpinCount modules implemented in ESRStudio software (Bruker patent). The singlet oxygen concentration was graphed as averages of three independent experiments ± SEM. The time-course graph was further analyzed with Nonlinear Regression using Graphpad Prism 9.4.1 to generate the following fitting curve (red) with an equation.

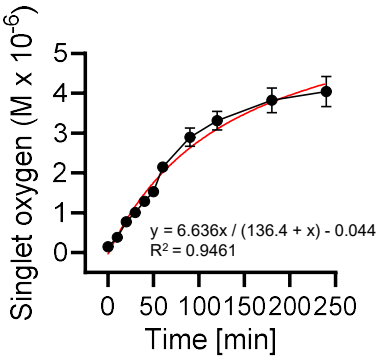

Table S1. ^{1}H, ^{13}C, and 2D [^{1}H-^{1}H COSY, ^{1}H-^{13}C HMBC (pulse sequence optimized for $^{n}J_{CH}$ = 8 Hz and 2 Hz), ROESY, and ^{1}H-^{15}N HMBC] NMR data for compound (±)-**1** in DMSO-d_6 (600 MHz for ^{1}H and 150 MHz for ^{13}C, respectively, δ ppm)

No.	δ_C	δ_N	δ_H (J in Hz)	^{1}H-^{1}H COSY	^{1}H-^{13}C HMBC (8 Hz)	^{1}H-^{13}C HMBC (2 Hz)	^{1}H-^{15}N HMBC	ROESY
1		n.d.						
2	139.5							
2a	121.4							
2b	123.2							
3	123.9		6.30, br d	4	2a, 5, 6a			
4	127.5		6.74, t (8.2)	3, 5	2b, 6			
5	126.2		7.41, t (8.2)	4, 6	3, 6a	3, 6a		
6	131.3		8.15, d (8.2)	5	2b, 4	2b, 4	7	
6a	144.2							
7		290.0						
7a	139.0							
7b	159.0							
8		110.2	10.29, br s	9	7a, 9, 10, 11a	7b, 9, 10, 11a, 12		
9	38.6		3.75, m	8, 10	7b, 11	7b, 11		
10	37.1		2.56, m	9	9, 11	9, 11	8	
11	187.8							
11a	104.3							
12	153.6							
12a	125.2							
12b	124.6							
13		124.9						
14	47.8		3.35, s		12, 15	12, 15	13	
15	44.7		3.89, s		12, 14	12, 14	13	
1'		141.3	10.37, s		2', 2a',12a', 12b'	2, 12b, 2', 2a', 2b', 7a', 12a', 12b'	1'	15'
2'	168.6							
2a'	136.3							
2b'	123.0							
3'	123.6		9.05, d (8.0)	4'	5', 2a', 2b', 6a'	5', 6', 2b', 6a'		
4'	131.5		8.14, t (8.0)	3', 5'	2b', 6'	2b', 6'		
5'	132.8		8.20, t (8.0)	4', 6'	3', 6a'	3', 6a'		
6'	130.1		8.43, d (8.0)	5'	2b', 4'	2', 2a', 2b', 4', 6a'		
6a'	148.5							
7'		n.d.						
7a'	143.8							
7b'	156.6							
8'		115.5	10.62, br s	9'	7a', 10', 11a'			
9'	39.4		3.74, m 3.64, m	8', 10'	7b', 10', 11'	7b', 11'		
10'	35.2		2.52, m 2.39, m	9'	9', 11', 11a'	9', 11', 11a'		
11'	184.4							
11a'	102.8							
12'	174.8							
12a'	70.3							
12b'	137.4							
13'		169.1						
14'	49.5		3.39, s		12', 15'	2, 11', 11a', 12', 12a', 12b', 15'	13'	
15'	44.7		3.95, s		12', 14'	2, 7b', 11', 11a', 12', 12a', 12b', 14'	13'	1'

n.d., not detected

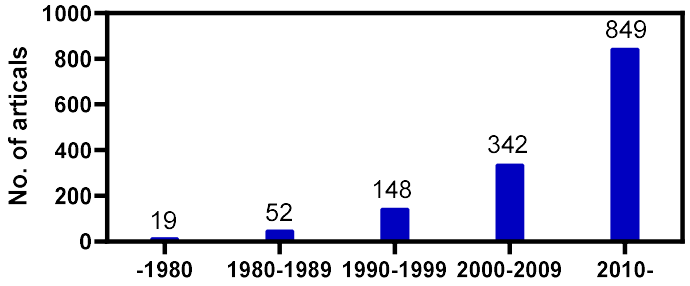

Figure S1. Reports on dimeric natural products in the past 40 years. "Dimeric natural products" was used as a keyword and searched in SciFinder.

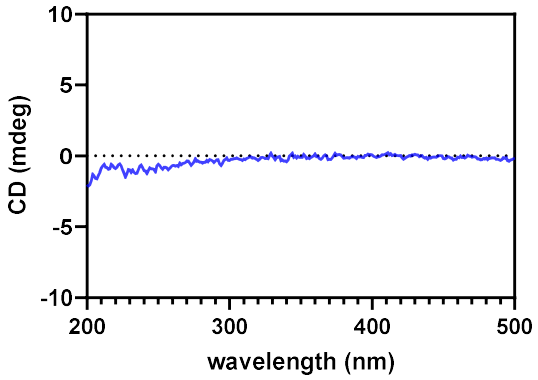

Figure S2. Experimental ECD spectrum of (±)-**1**.

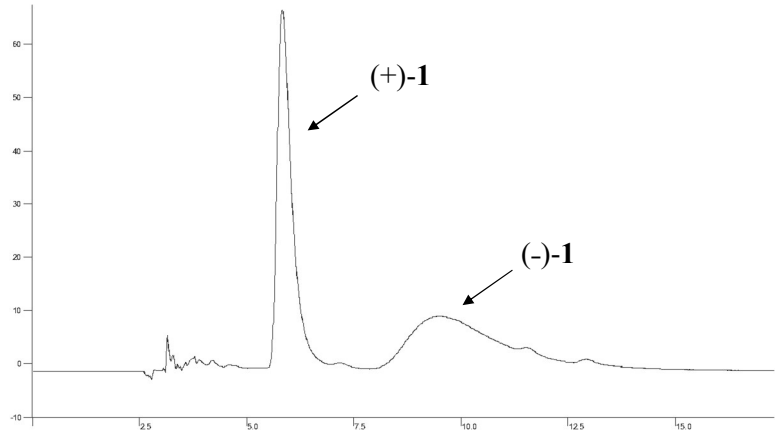

Figure S3. Chiral-phase HPLC analysis of (±)-**1** [HPLC conditions: Lux 5 μm i-Amylose-3 column (100 Å, 250 × 4.6 mm) with flow rate of 1 mL/min (eluted with 40% MeCN with 0.1% TFA)].

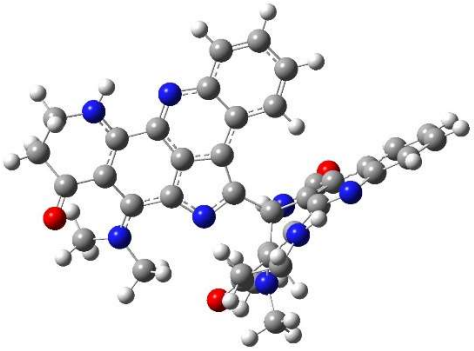

Conformer 1, RE = 1.7 kcal/mol (1.9 %)

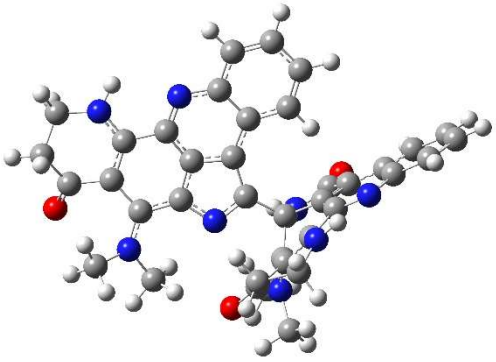

Conformer 2, RE = 1.9 kcal/mol (1.5 %)

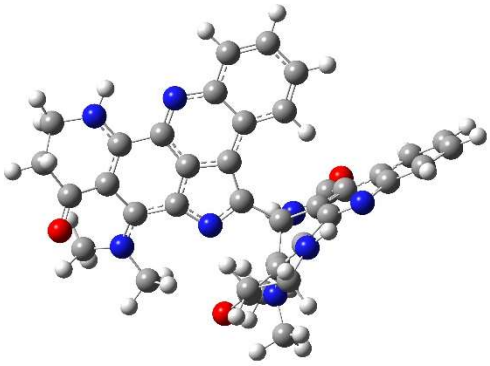

Conformer 3, RE = 0 kcal/mol (37.6 %)

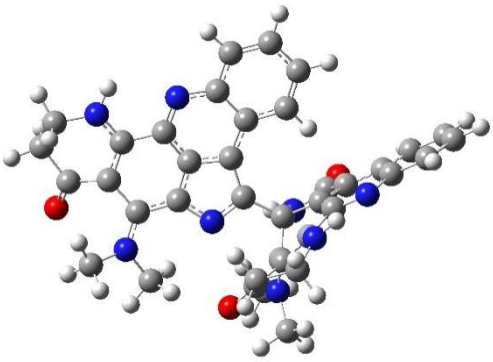

Conformer 4, RE = 0.1 kcal/mol (32.1 %)

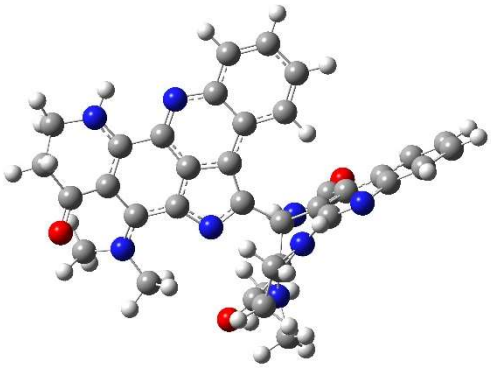

Conformer 5, RE = 0.6 kcal/mol (14.6 %)

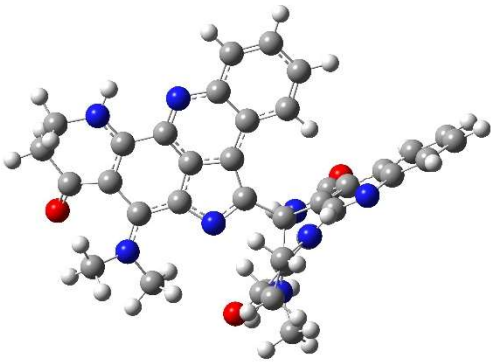

Conformer 6, RE = 0.7 kcal/mol (12.2 %)

Figure S4. Optimized conformers of the 12a'*S* isomer of (±)-**1** at the DGDZVP level in MeOH

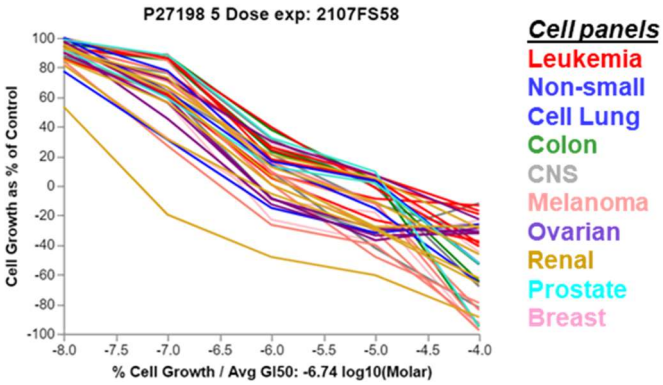

Figure S5. Dose-response curves of **2** in the NCI-60 Human Tumor Cell Lines Screen

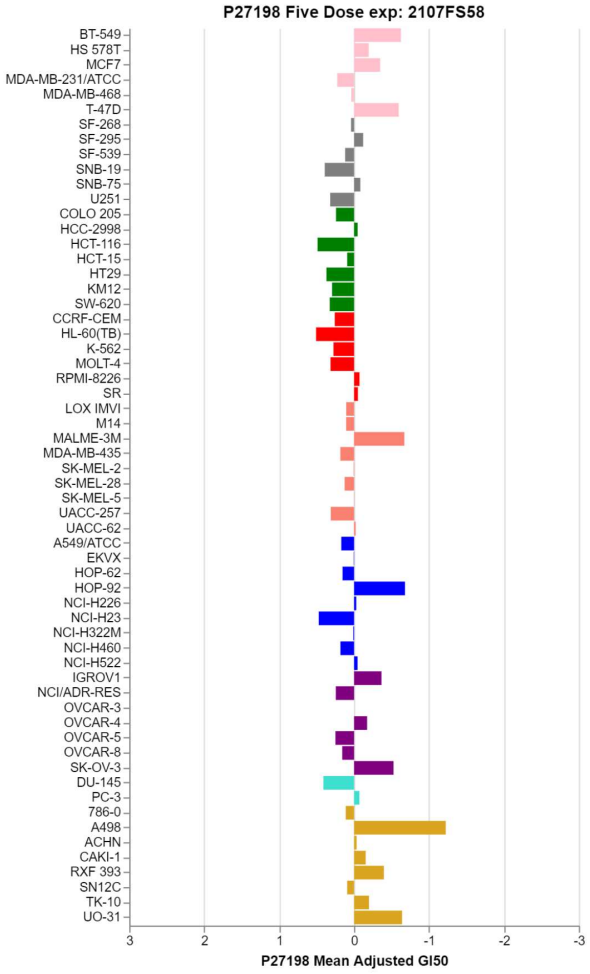

Figure S6. Mean graph of the NCI-60 cell line screening data for **2**. Zero on the X-axis represents the mean GI_{50} value of 0.18 μM against all of the cell lines tested. Bars to left represent cell lies that had GI_{50} values less potent than the mean, while the bars to the right represent cell lies that had GI_{50} values more potent than the mean value.

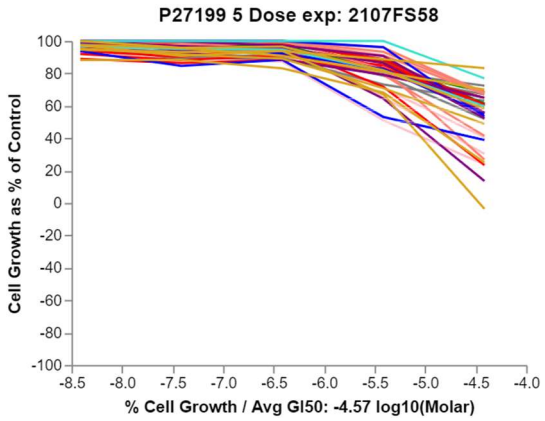

Figure S7. Dose-response curves of (+)-**1** in the NCI-60 Human Tumor Cell Lines Screen

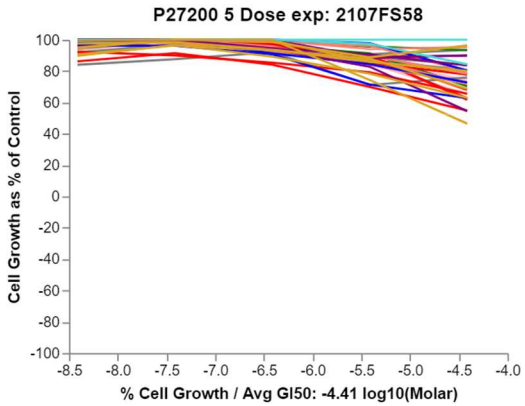

Figure S8. Dose-response curves of (-)-**1** in the NCI-60 Human Tumor Cell Lines Screen

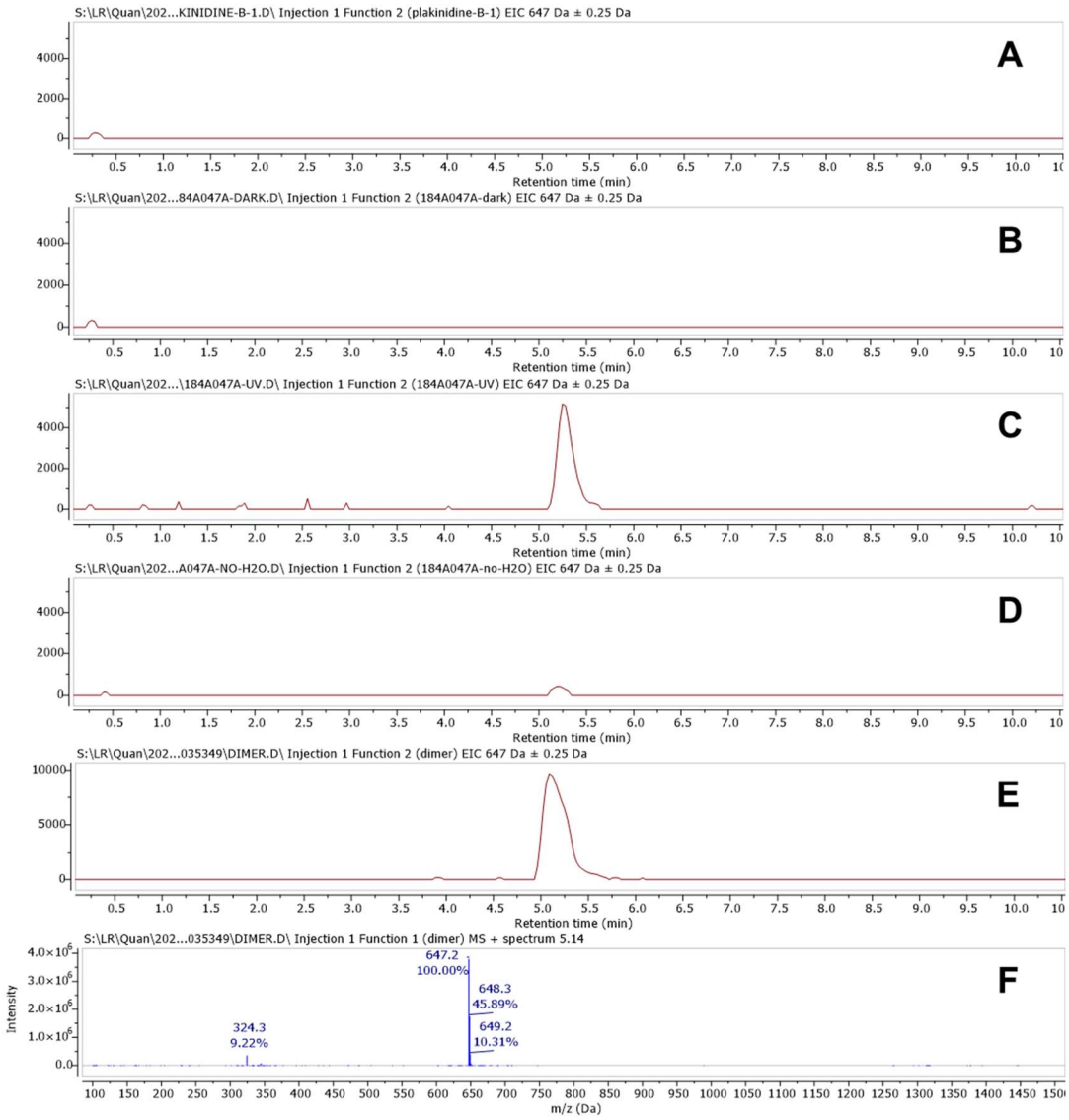

Figure S9. LCMS analysis for investigating the effects of light and solvents on the dimerization of **2**. **A**–**E**: selected ion traces for *m*/*z* 647 ± 0.25 Da in the ESI^+ mode. **A.** purified **2**; **B**. reaction of **2** in MeCN/H_2O (1:1) in darkness; **C**. reaction of **2** in MeCN/H_2O (1:1) with UV irradiation; **D.** reaction of **2** in anhydrous MeCN with UV irradiation; **E.** purified (±)-**1**. Reaction conditions: Compound **2** (0.1 mg) was stirred in a 100 µL solvent at room temperature for 4 h prior to direct analysis by LCMS. UV irradiations were applied using a Mineralight® UVSL-25 lamp (4-watt) at 366 nm. **F**, $ESIMS^+$ spectrum of (±)-**1**.

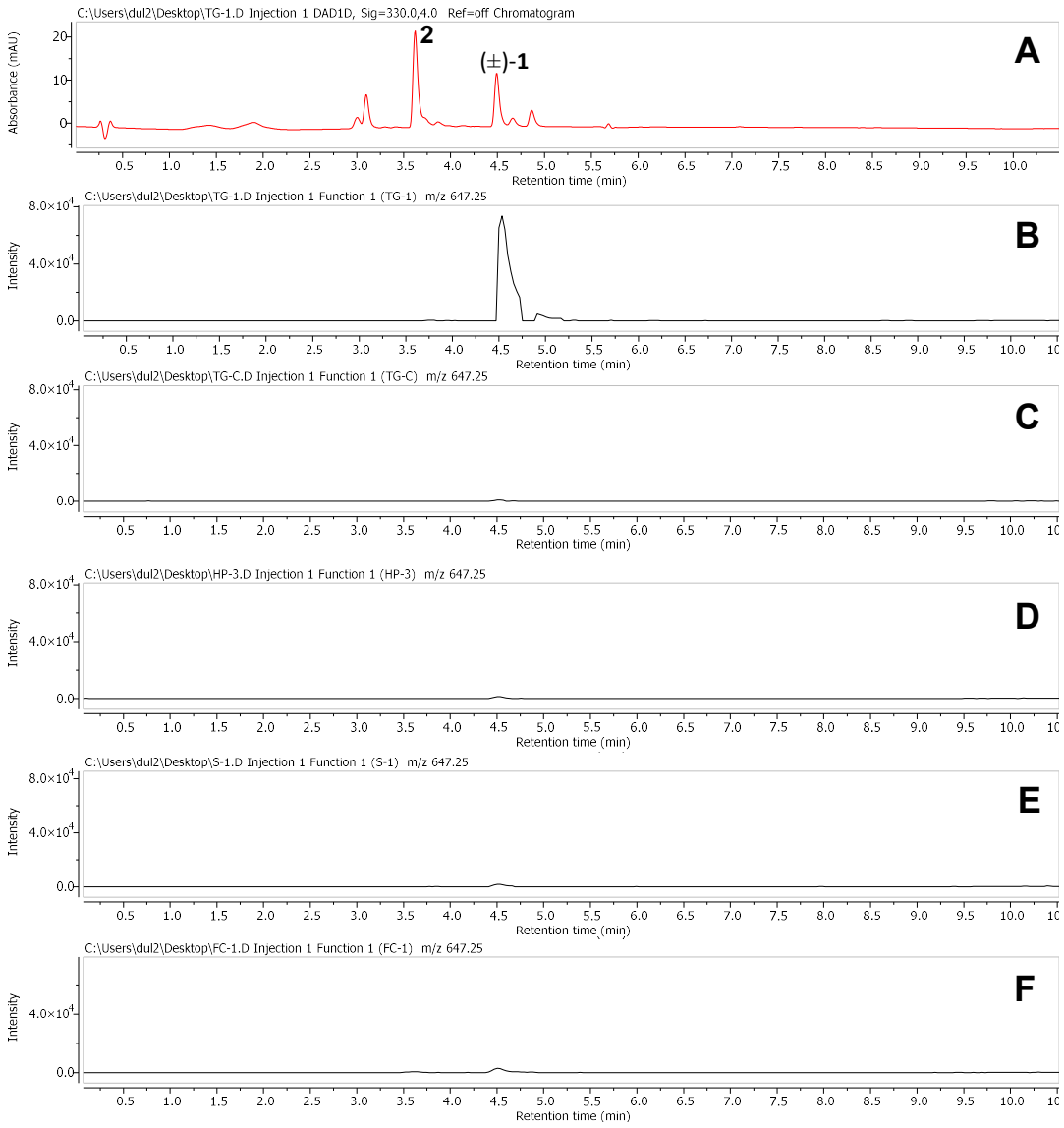

Figure S10. LCMS-PDA analysis of the ROS studies. **A.** UV (330 nm) chromatogram; **B–G**: selected ion traces for *m/z* 647.25 Da in the ESI^+ mode. **A** & **B.** reaction of **2** with thermally regenerated $^1O_2$; **C**. **2** under the same reaction conditions of **A** and **B** without generation of $^1O_2$; **D**. reaction of **2** with H_2O_2; **E.** reaction of **2** with superoxide; **F.** reaction of **2** under Fenton conditions.

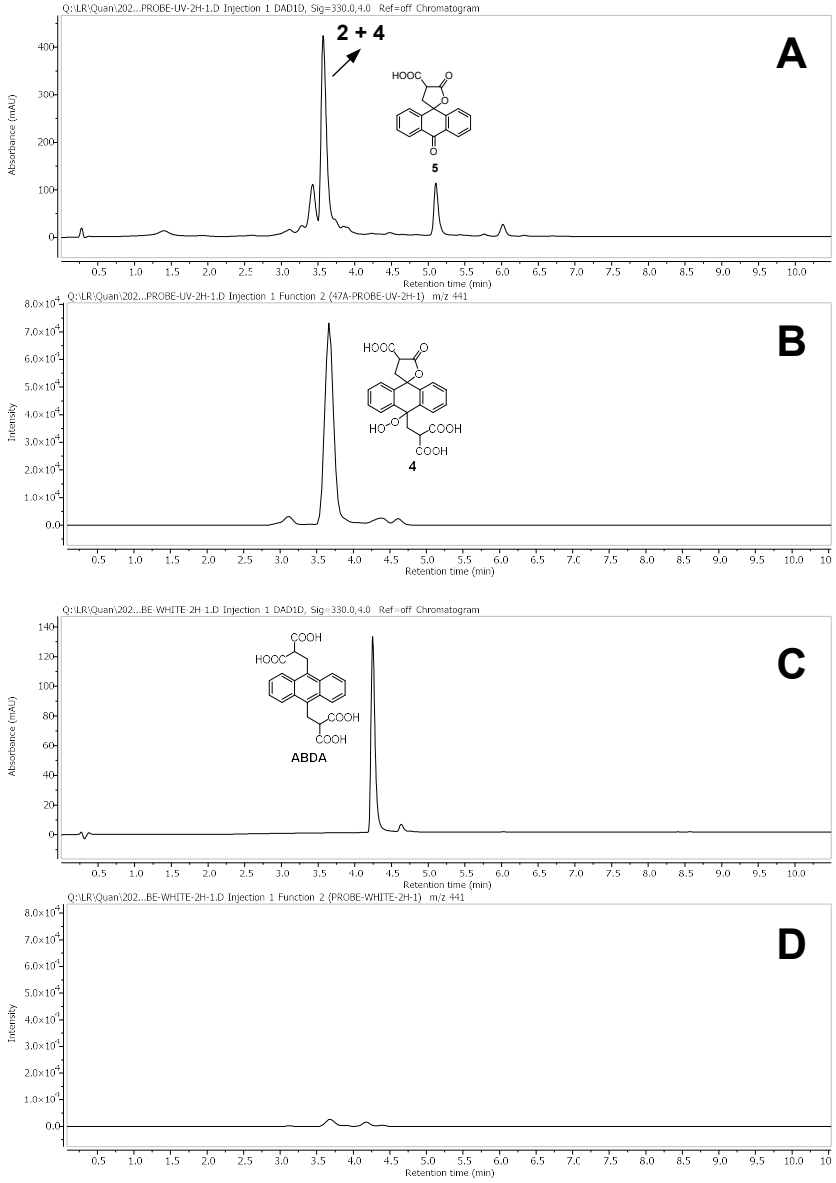

Figure S11. LCMS-PDA analysis of **2**-sensitized photooxidation of the $^1O_2$ probe ABDA. **A** & **C:** UV (330 nm) chromatogram; **B** & **D**: selected ion traces for *m*/*z* 441 Da in the ESI^- mode. **A** & **B.** reaction of ABDA in MeCN/H_2O (1:1) with the presence of **2** and white light (15 W LED) irradiation for 2 h; **C** & **D.** ABDA in MeCN/H_2O (1:1) with white light irradiation for 2 h.

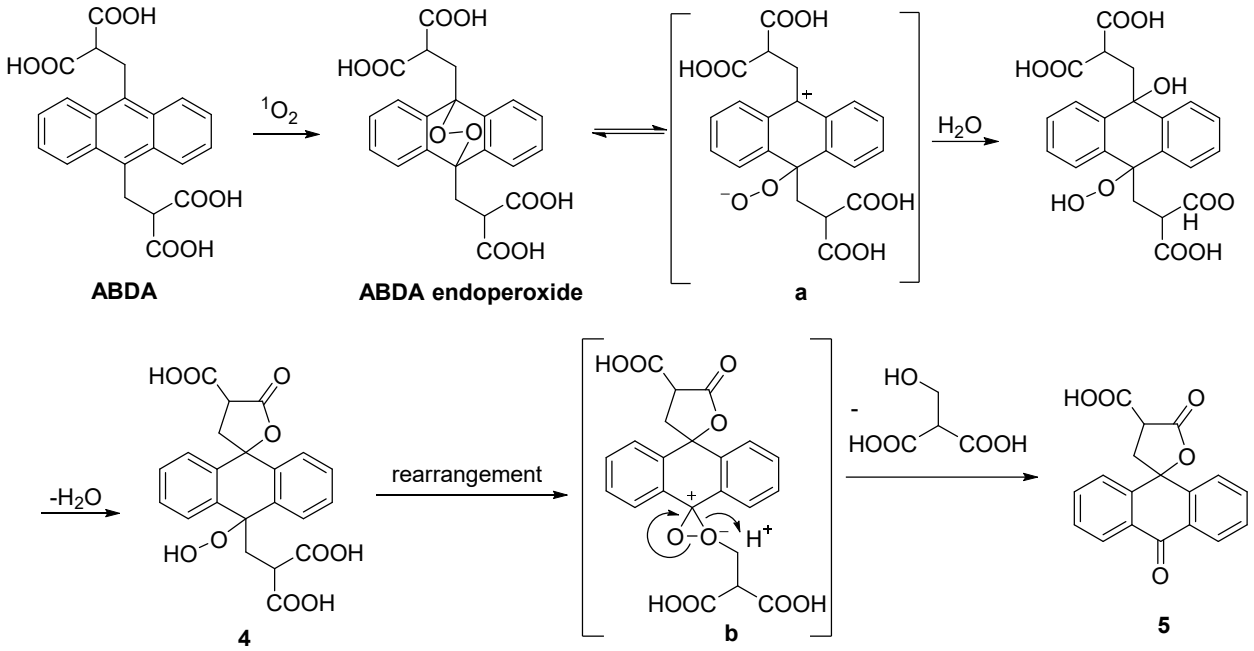

Figure S12. Proposed mechanism of **2**-sensitized photooxidation of the $^1O_2$ probe ABDA.

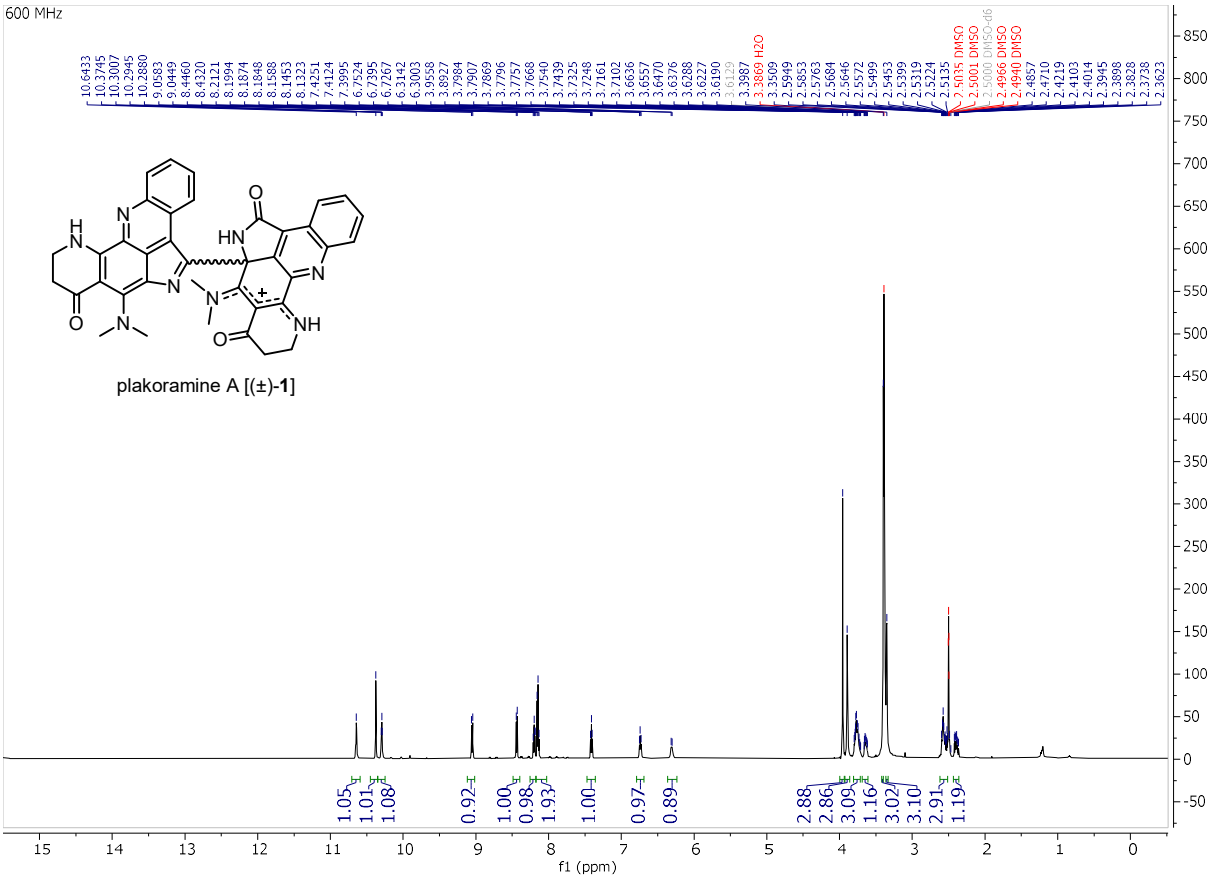

Figure S13. ^{1}H NMR spectrum of (±)-**1** in DMSO-d_6

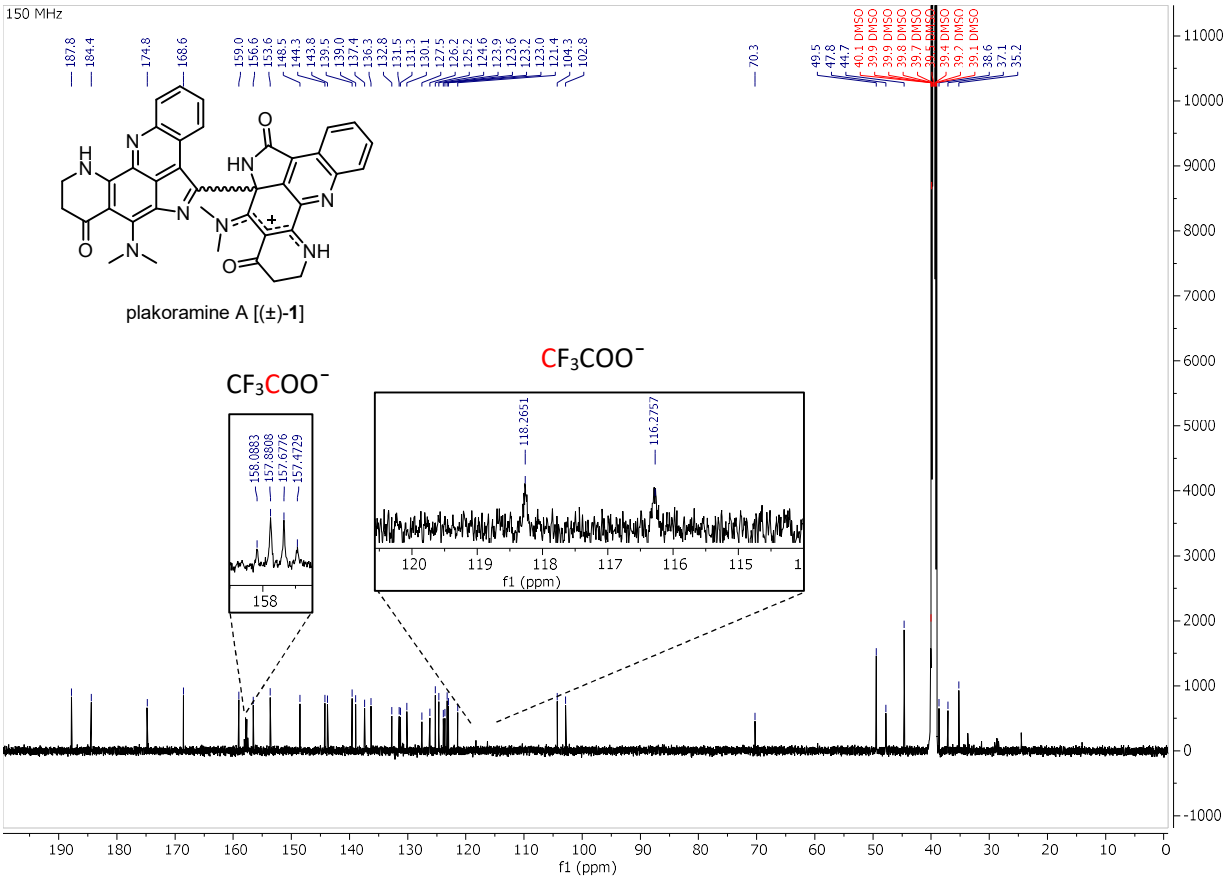

Figure S14. ^{13}C NMR spectrum of (±)-**1** in DMSO-d_6

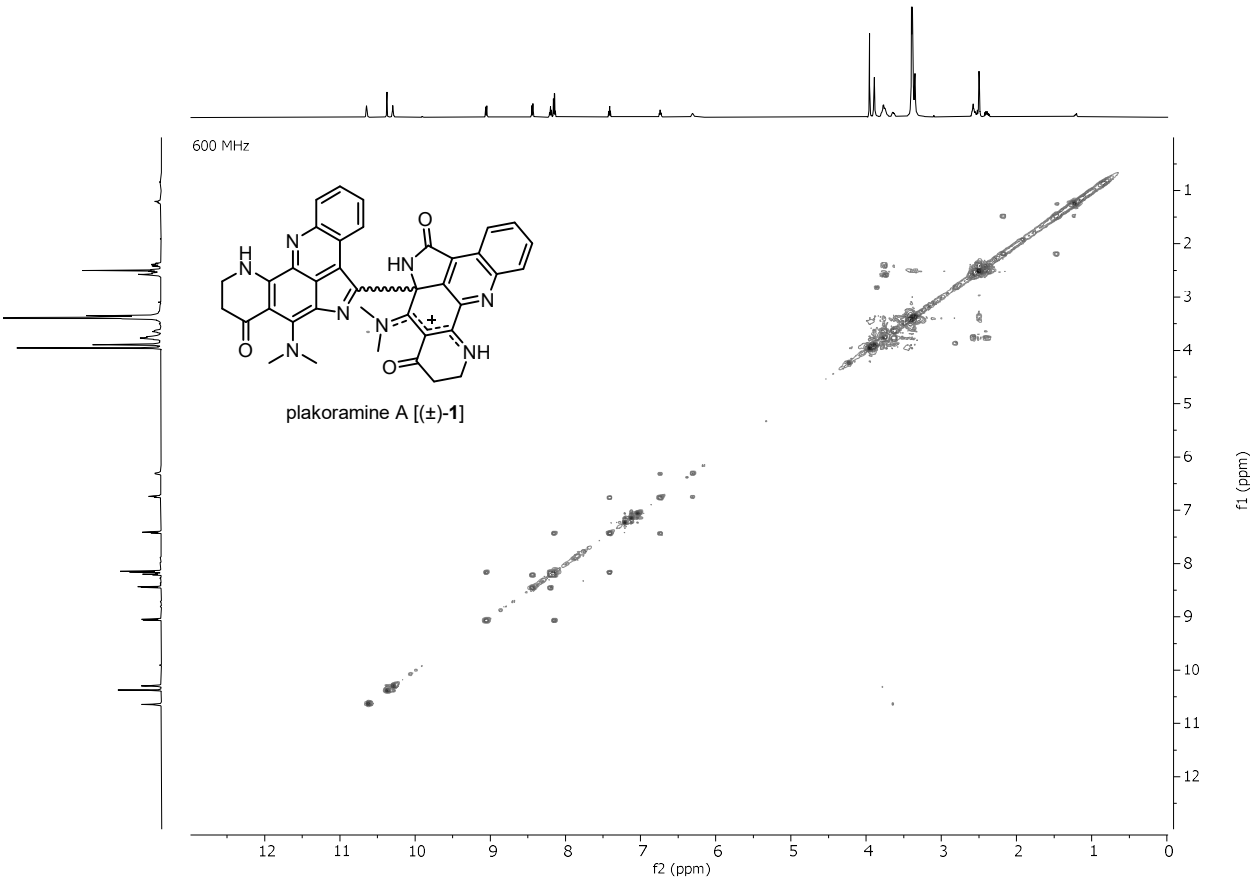

Figure S15. ^{1}H-^{1}H COSY spectrum of (±)-**1** in DMSO-d_6

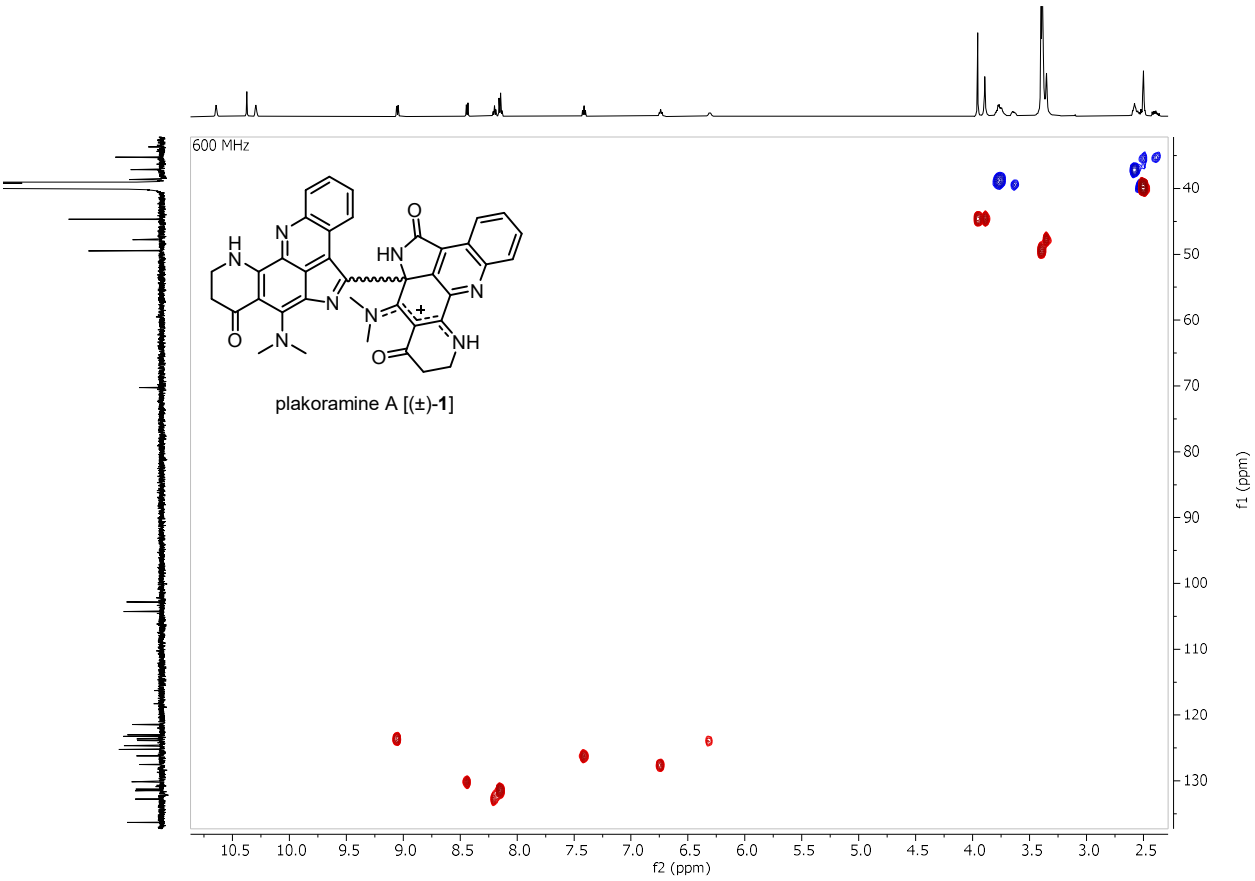

Figure S16. ^{1}H – ^{13}C HSQC spectrum of (±)-**1** in DMSO-d_6

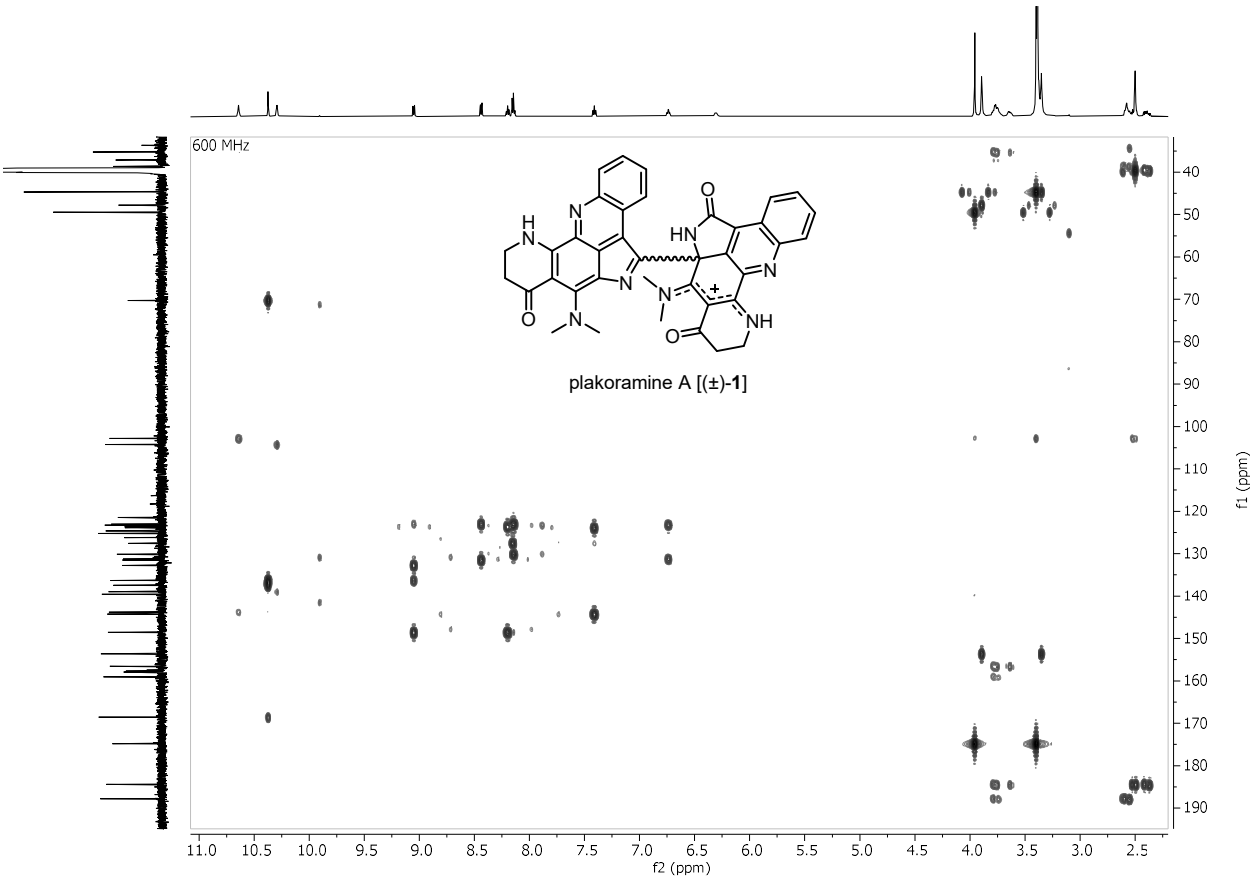

Figure S17. $^{1}H - {}^{13}C$ HMBC (pulse sequence optimized for $^{n}J_{CH}$ = 8 Hz) spectrum of (±)-**1** in DMSO-d_6

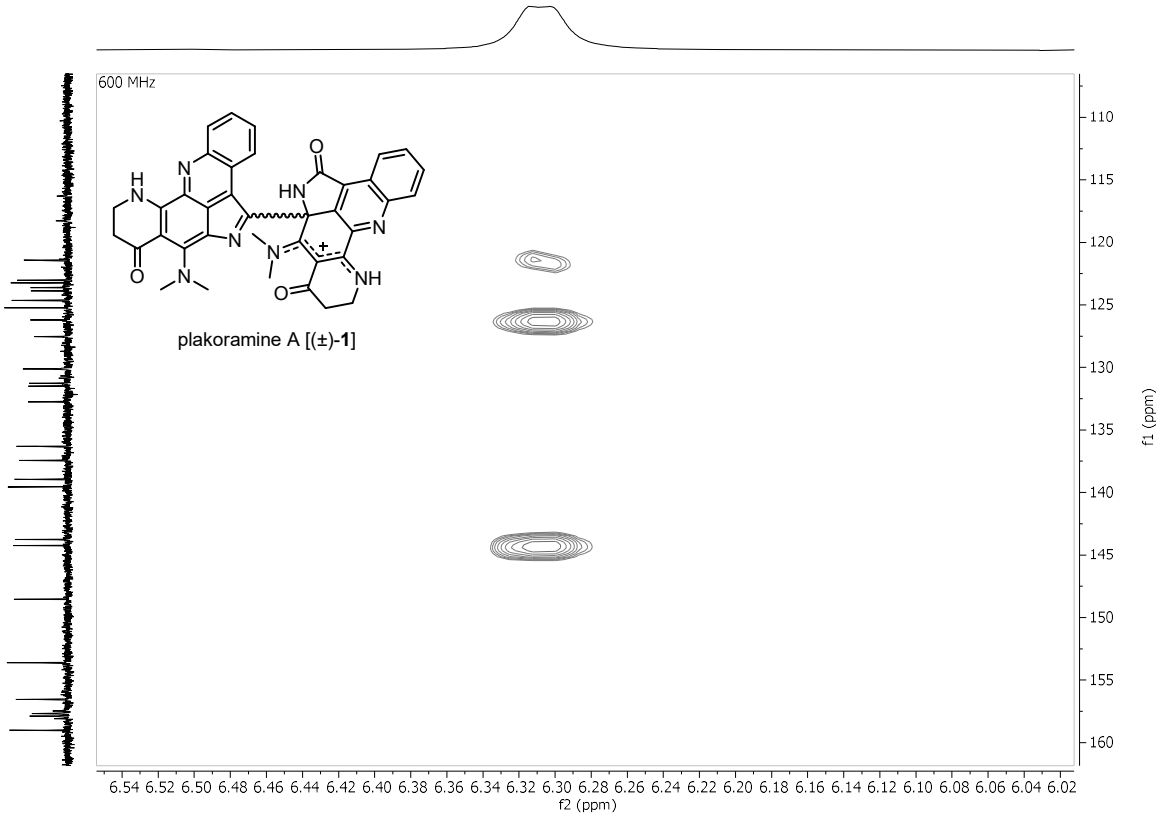

Figure S18. $^{1}H - {}^{13}C$ HMBC (pulse sequence optimized for $^{n}J_{CH}$ = 8 Hz, selected region) spectrum of (±)-**1** in DMSO-d_6

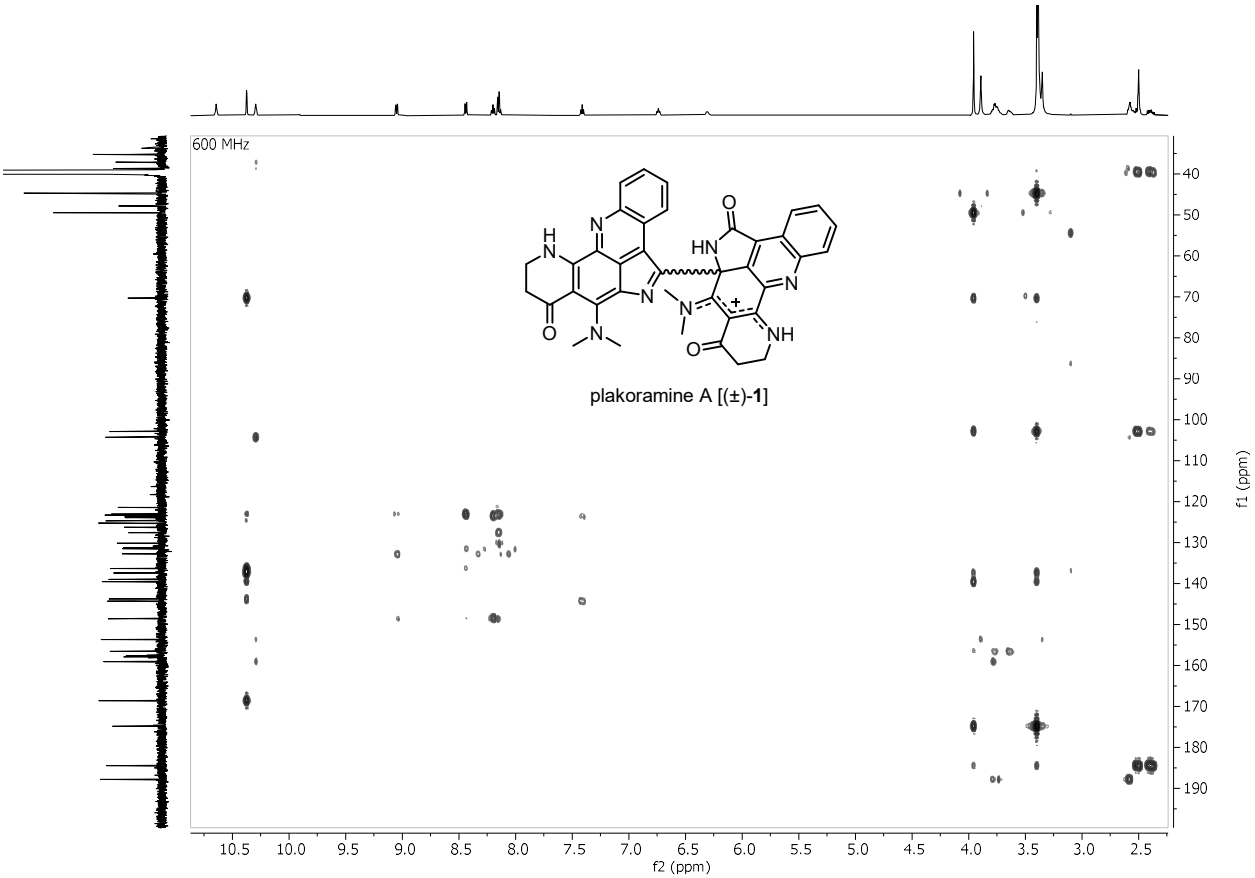

Figure S19. $^{1}H - {}^{13}C$ HMBC (pulse sequence optimized for $^{n}J_{CH} = 2$ Hz) spectrum of (±)-**1** in DMSO-d_6

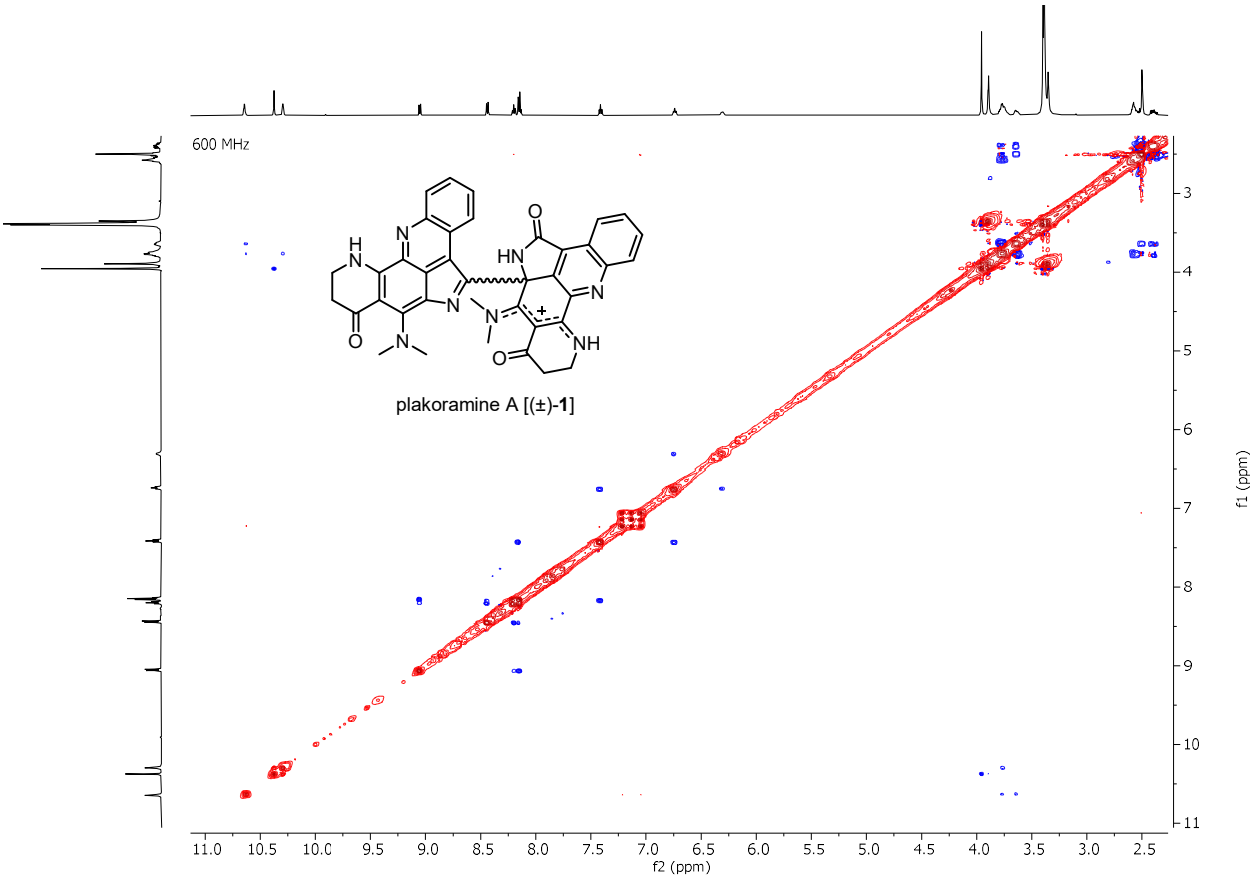

Figure S20. ^{1}H – ^{1}H ROESY spectrum of (±)-**1** in DMSO-d_6

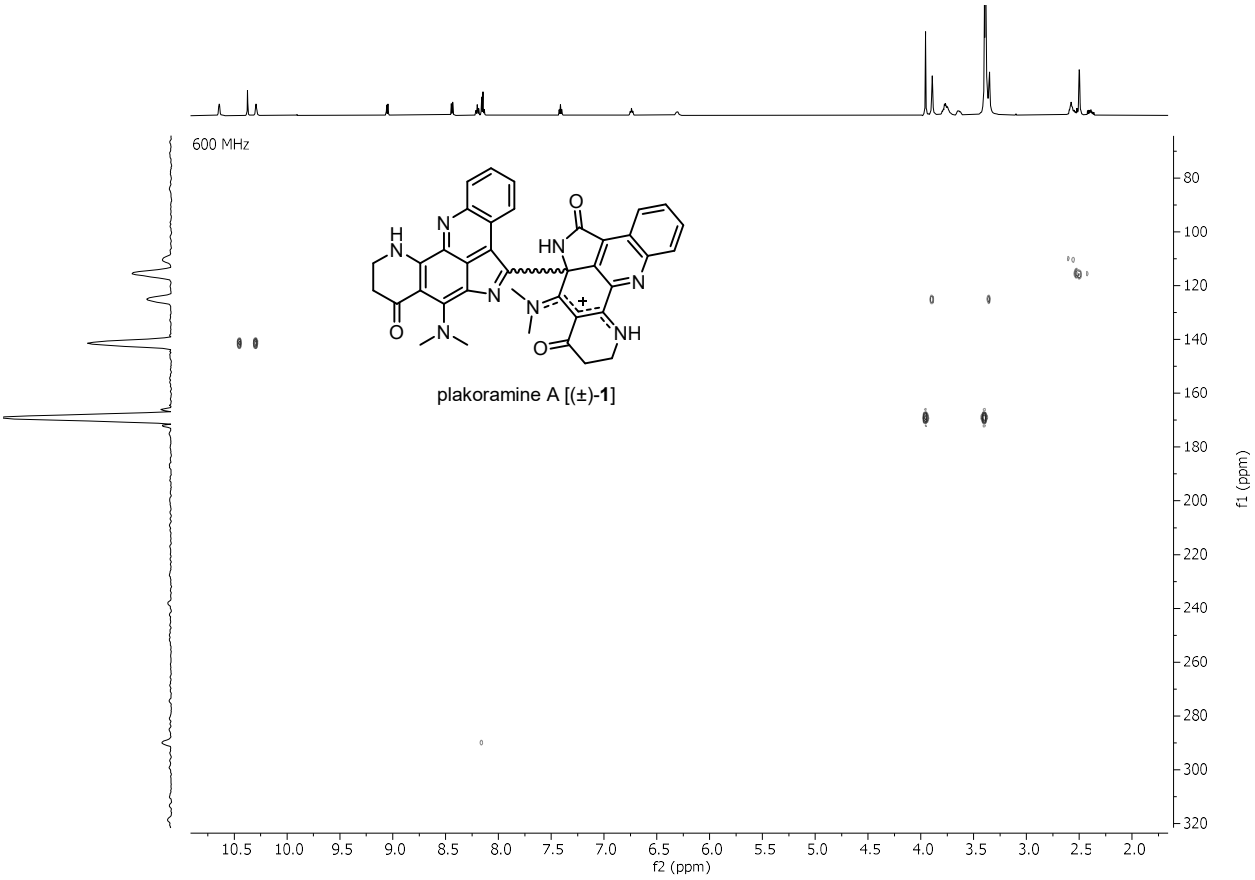

Figure S21. $^{1}H - {}^{15}N$ HMBC spectrum of (±)-**1** in DMSO-d_6

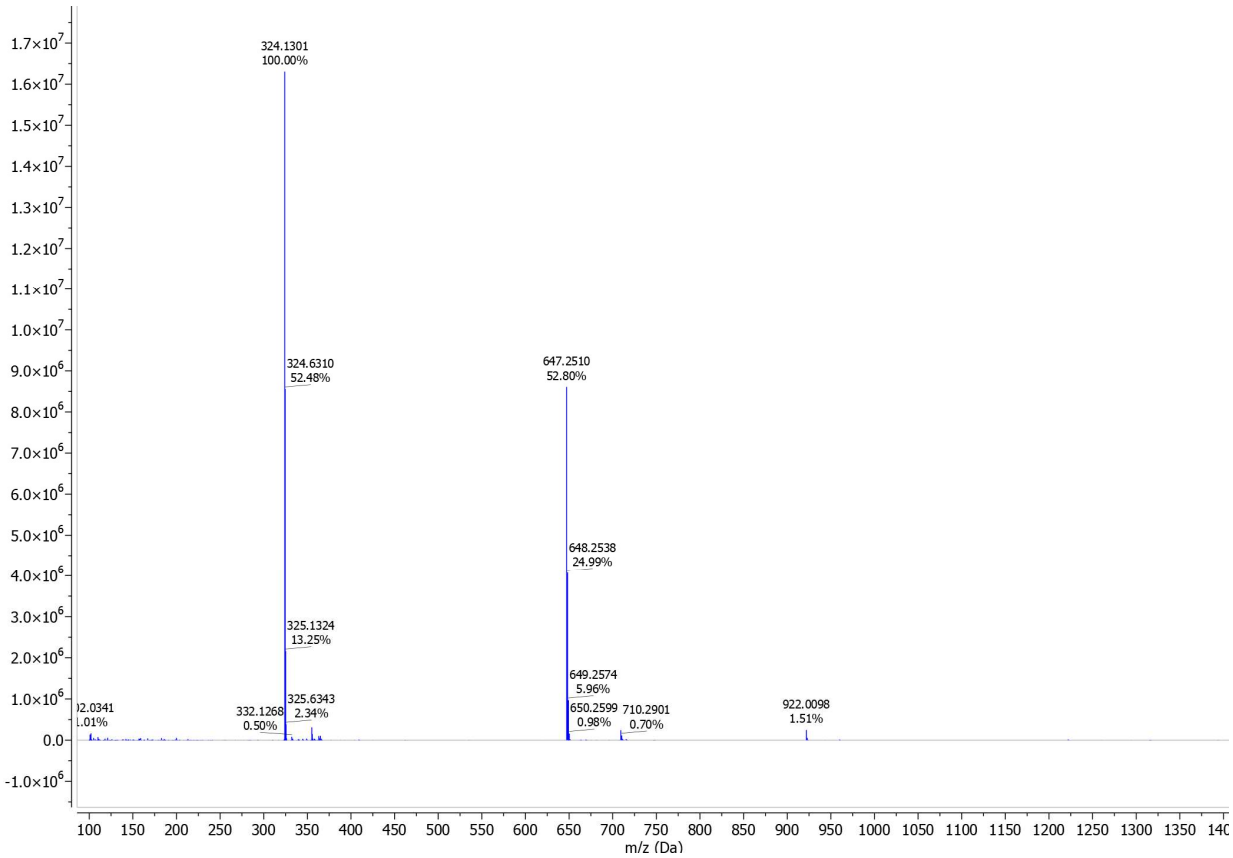

Figure S22. HRESIMS^{+} spectrum of (±)-**1**

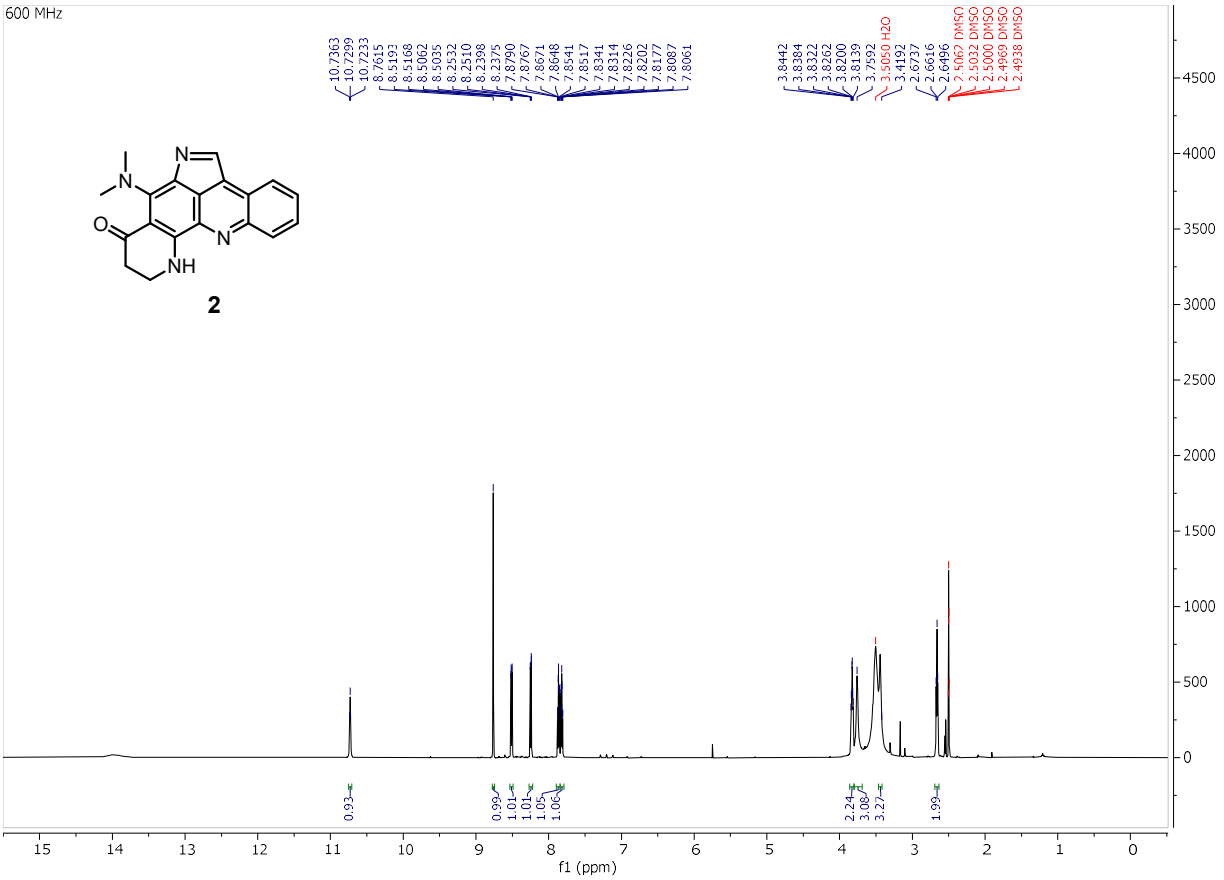

Figure S23. ^{1}H NMR spectrum of **2** in DMSO-d_6

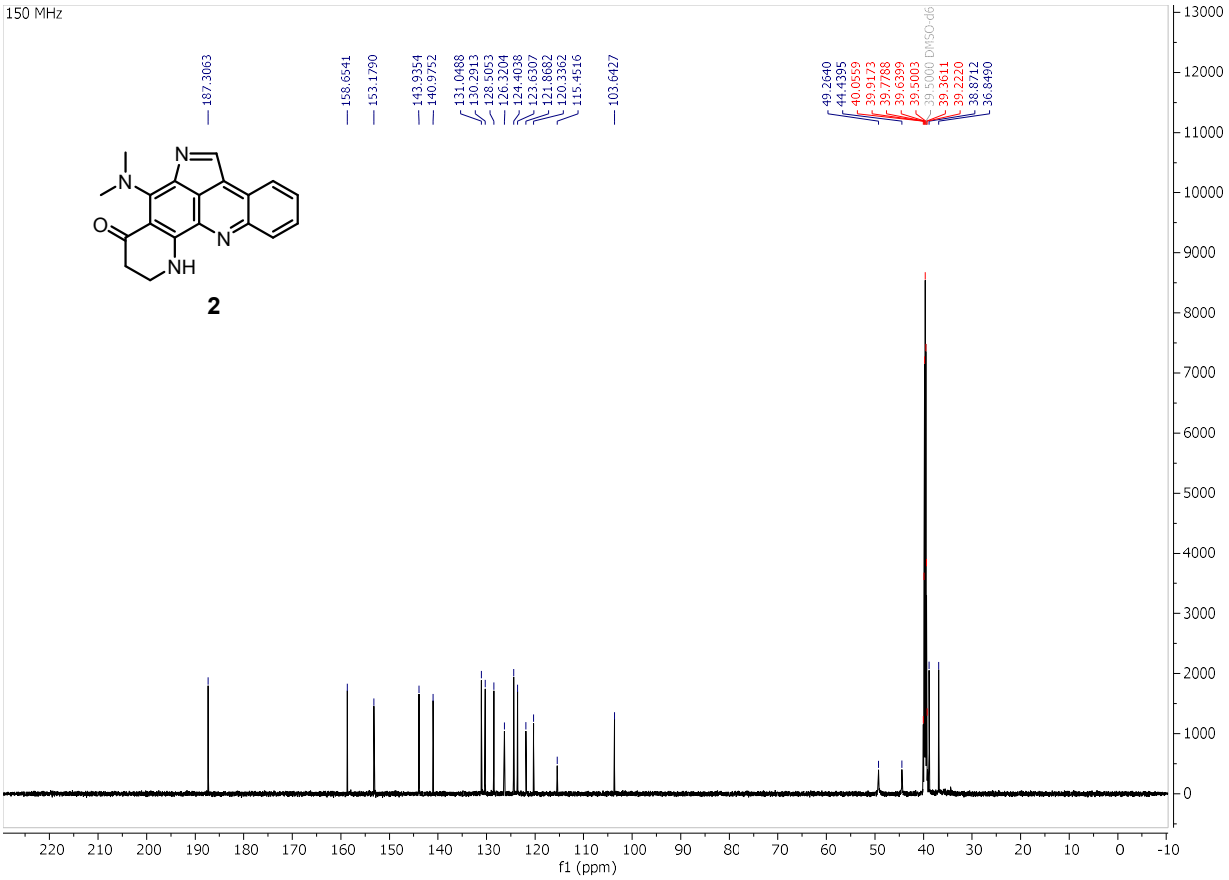

Figure S24. ^{13}C NMR spectrum of **2** in DMSO-d_6

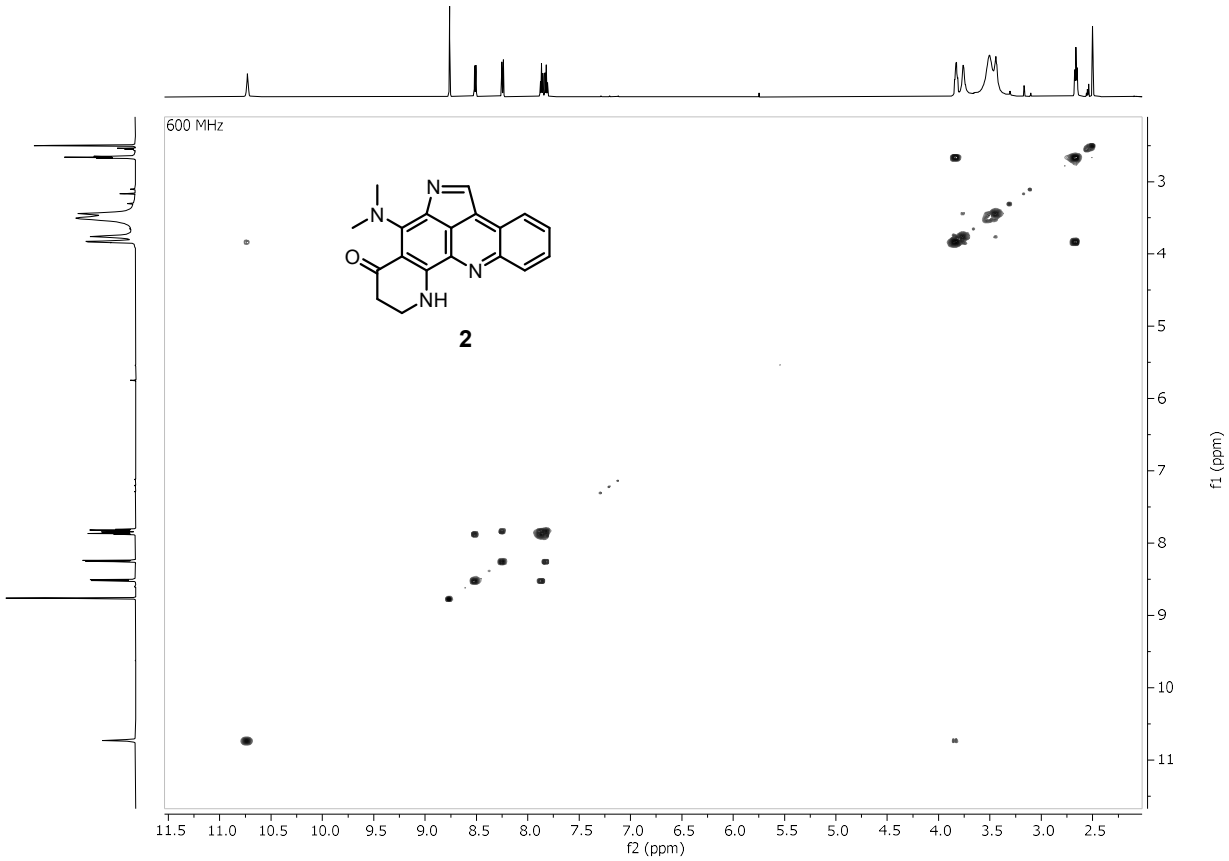

Figure S25. $^{1}H - {}^{1}H$ COSY spectrum of **2** in DMSO-d_6

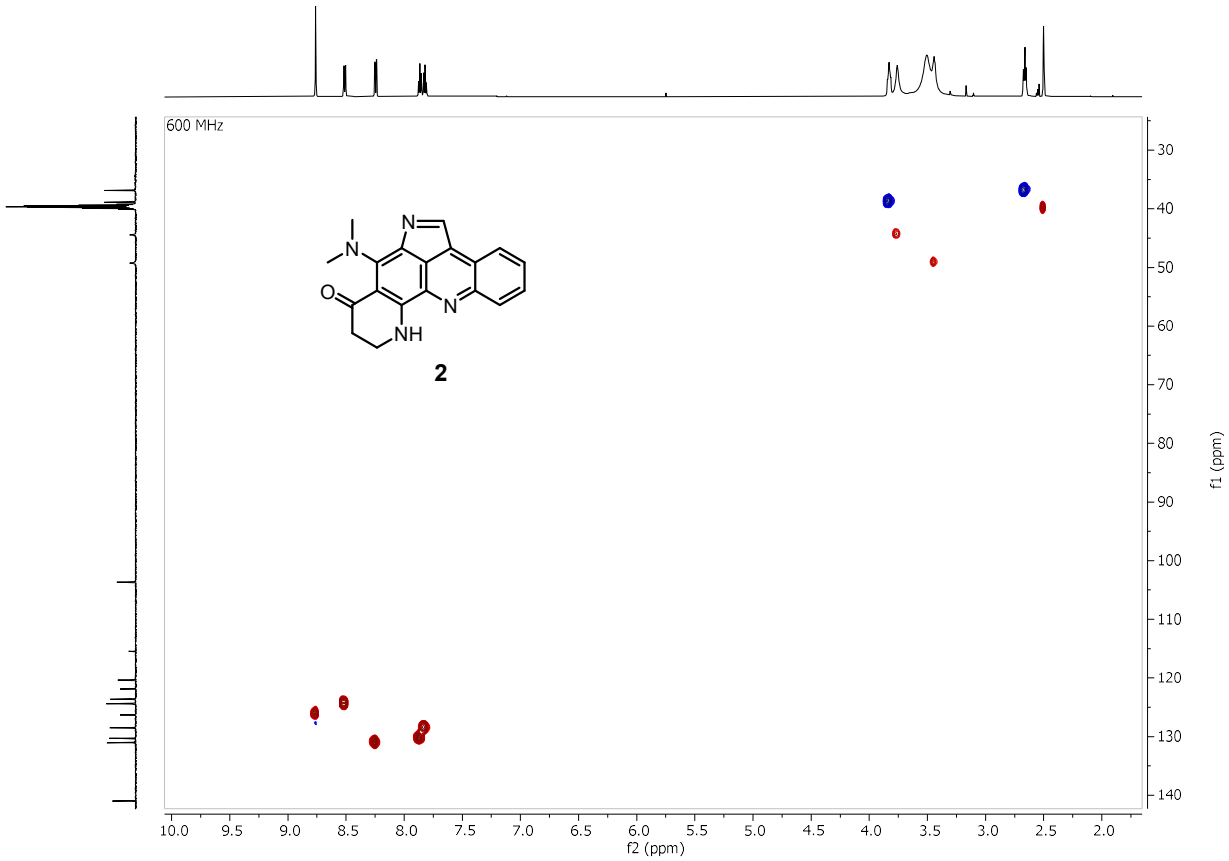

Figure S26. ^{1}H – ^{13}C HSQC spectrum of **2** in DMSO-d_6

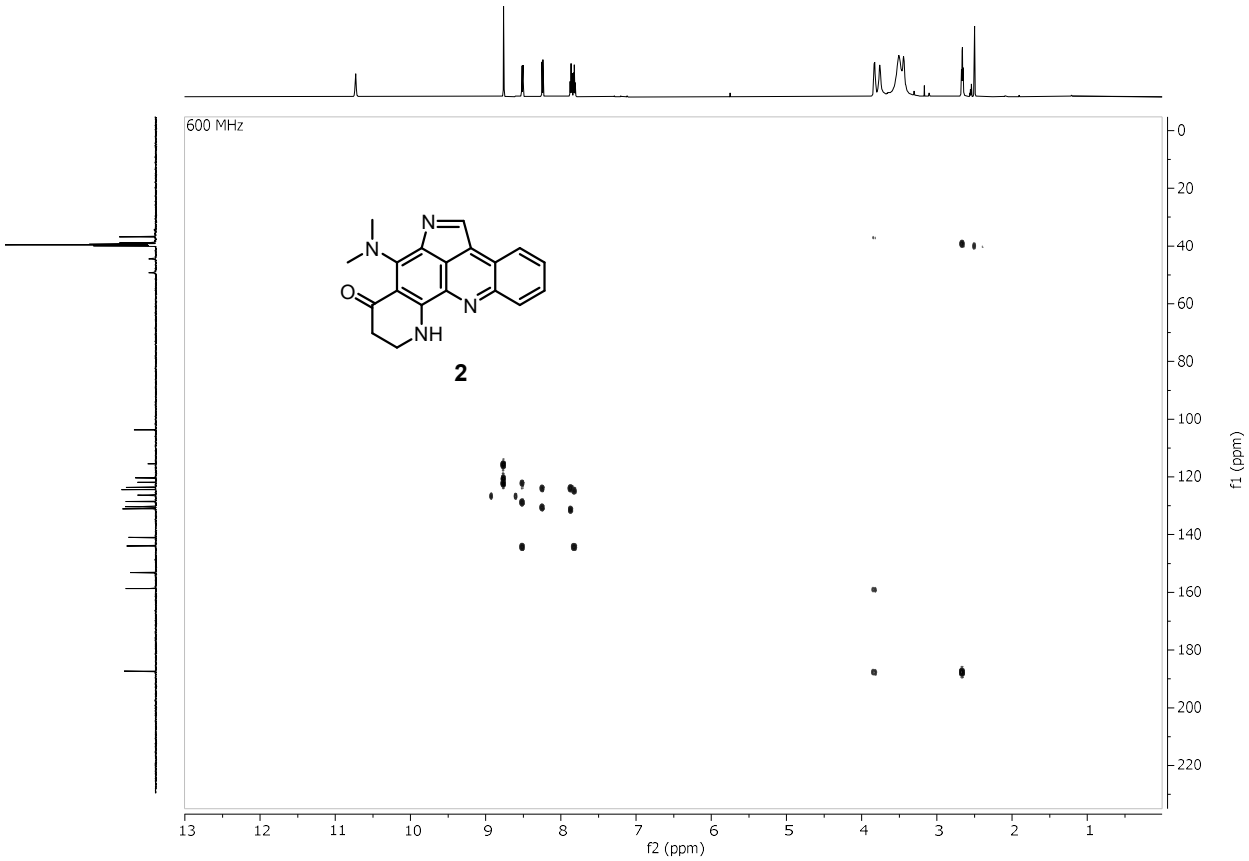

Figure S27. ^{1}H – ^{13}C HMBC spectrum of **2** in DMSO-d_6

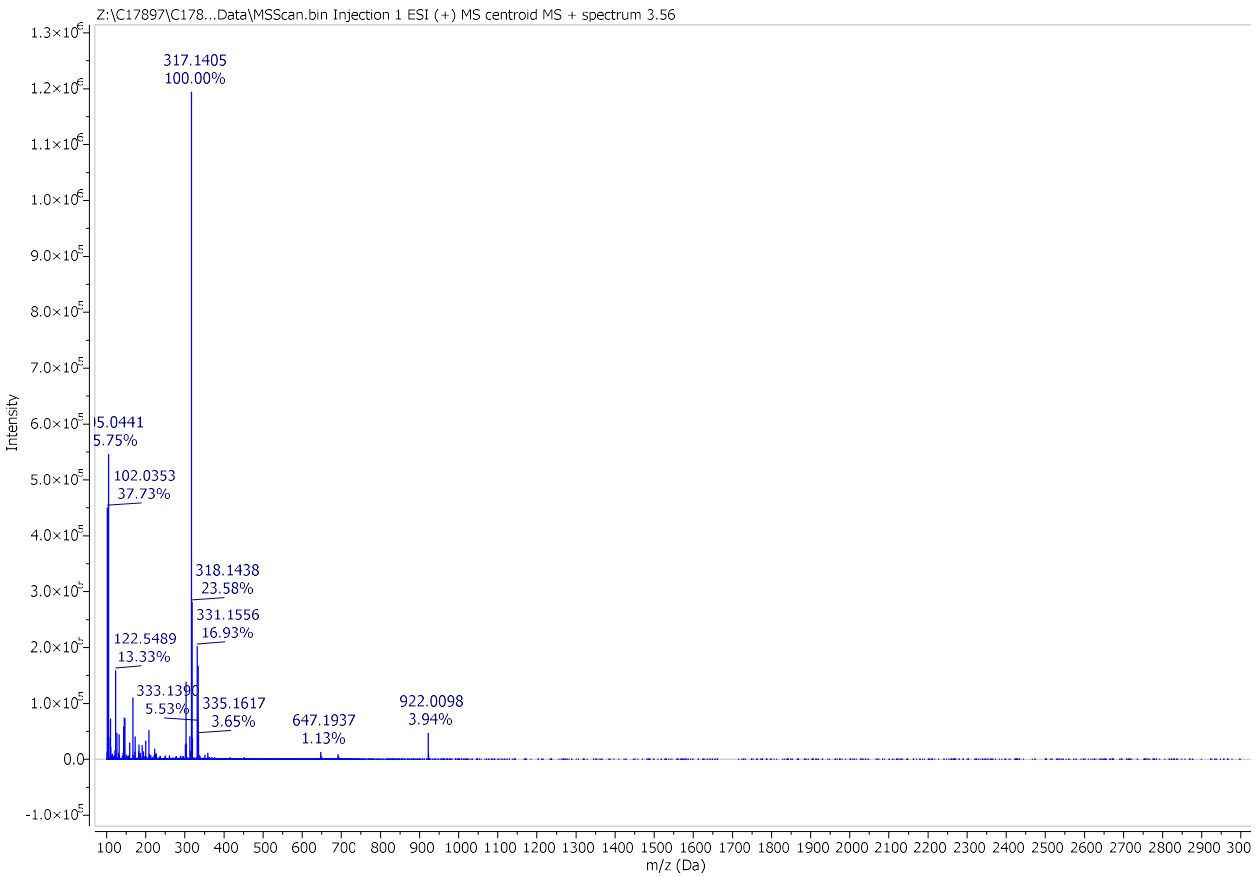

Figure S28. HRESIMS^{+} spectrum of **2**

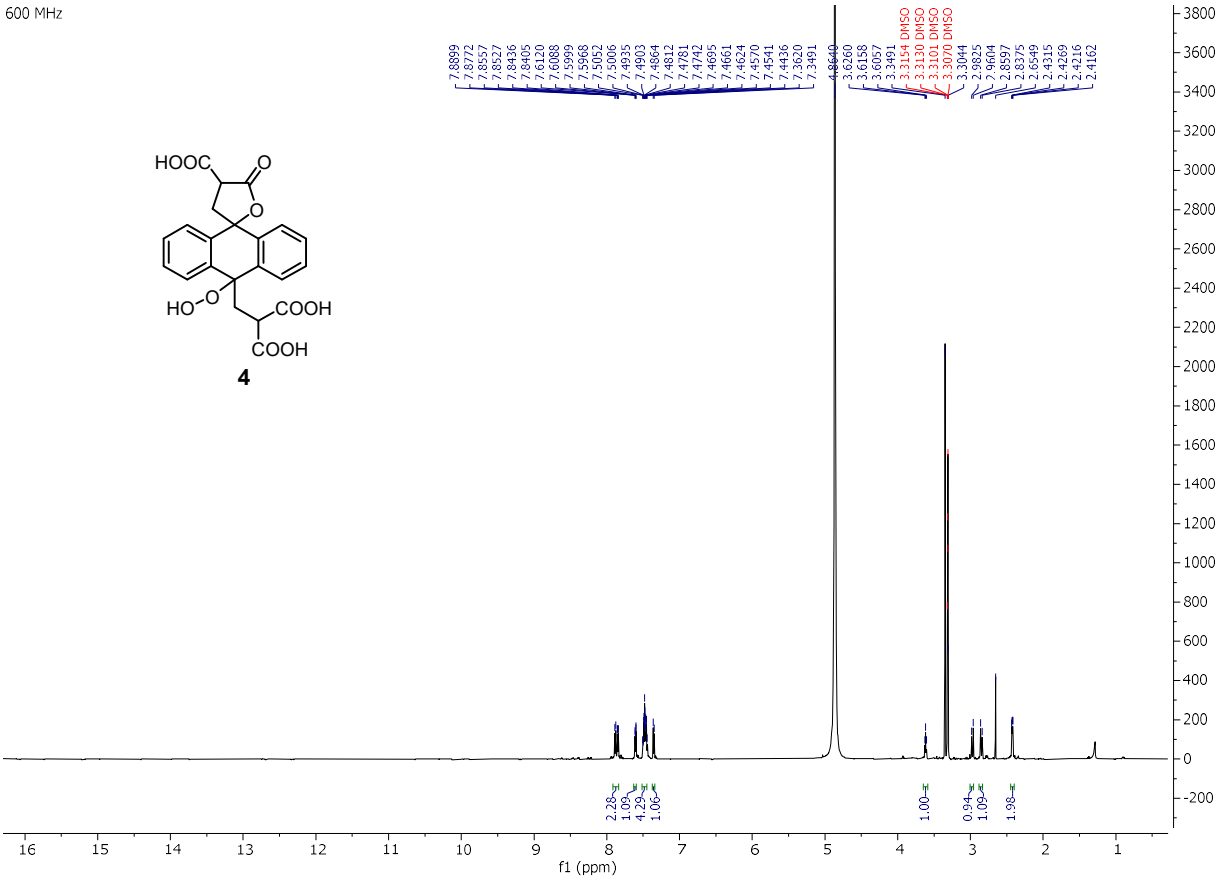

Figure S29. ^{1}H NMR spectrum of **4** in Methanol-d_4

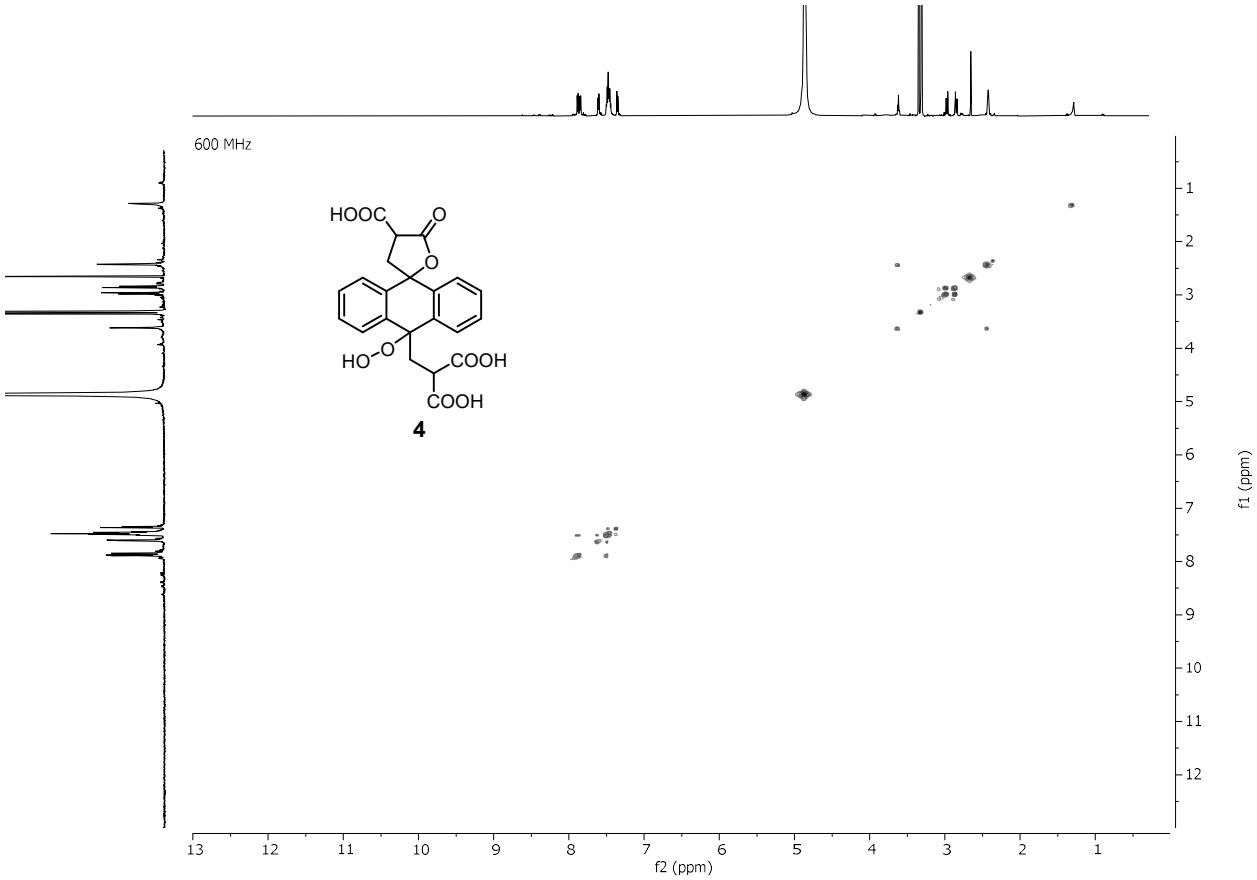

Figure S30. $^{1}H - {}^{1}H$ COSY spectrum of **4** in Methanol-d_4

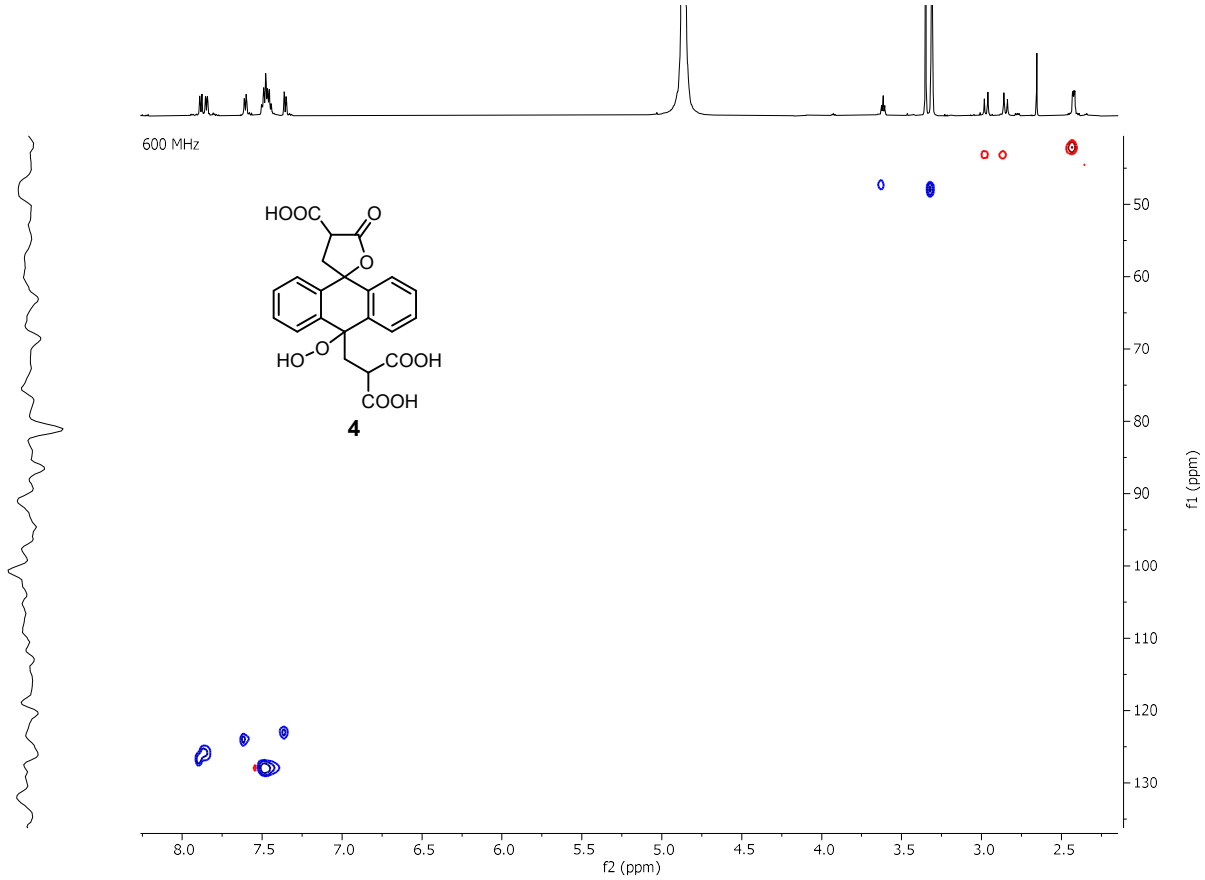

Figure S31. ^{1}H – ^{13}C HSQC spectrum of **4** in Methanol-d_4

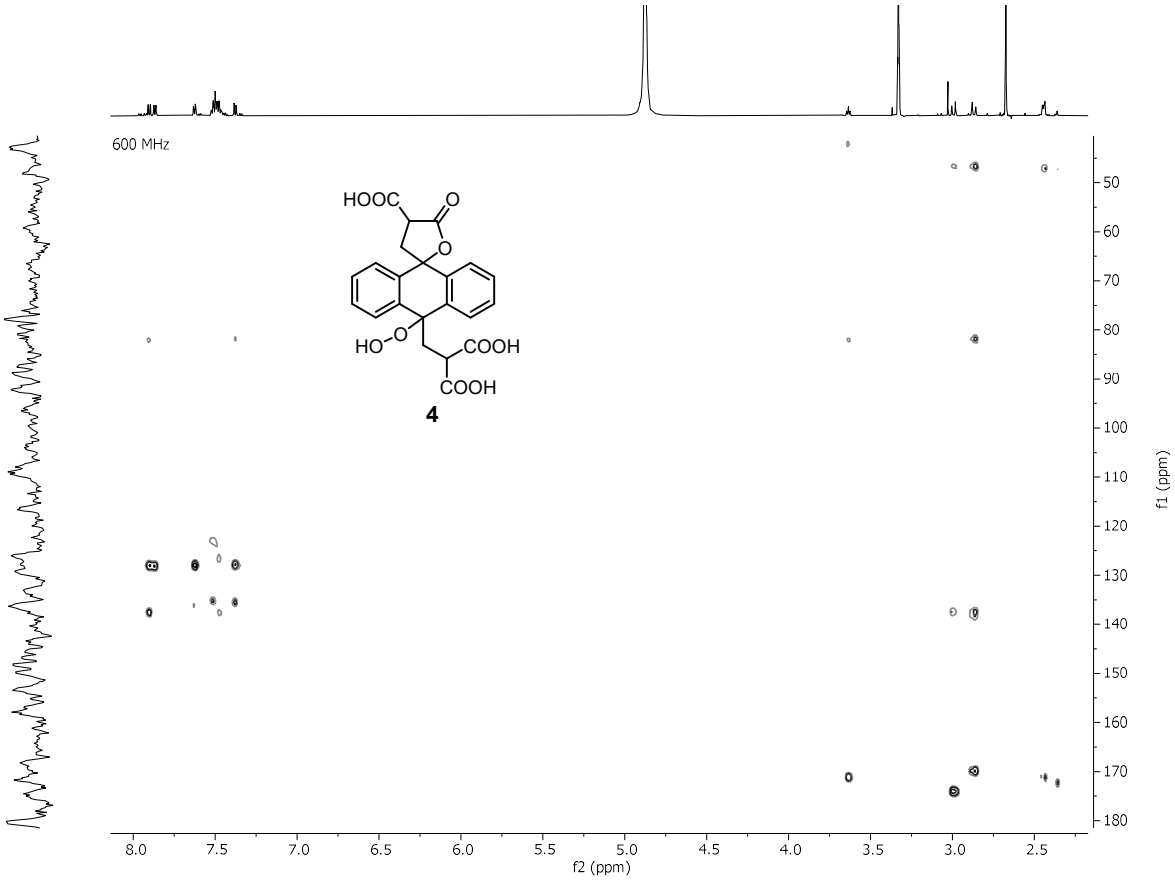

Figure S32. $^{1}H - {}^{13}C$ HMBC spectrum of **4** in Methanol-d_4

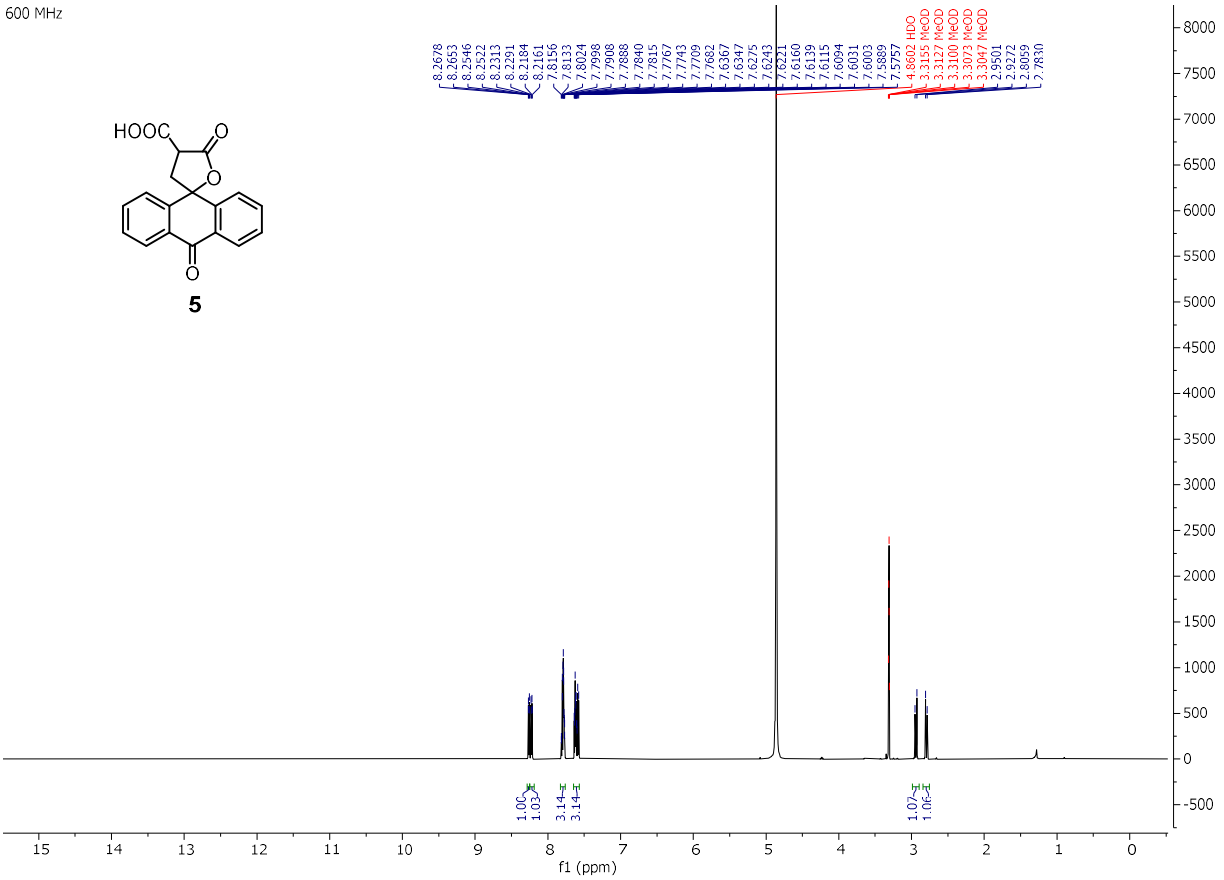

Figure S33. ^{1}H NMR spectrum of **5** in methanol-d_4

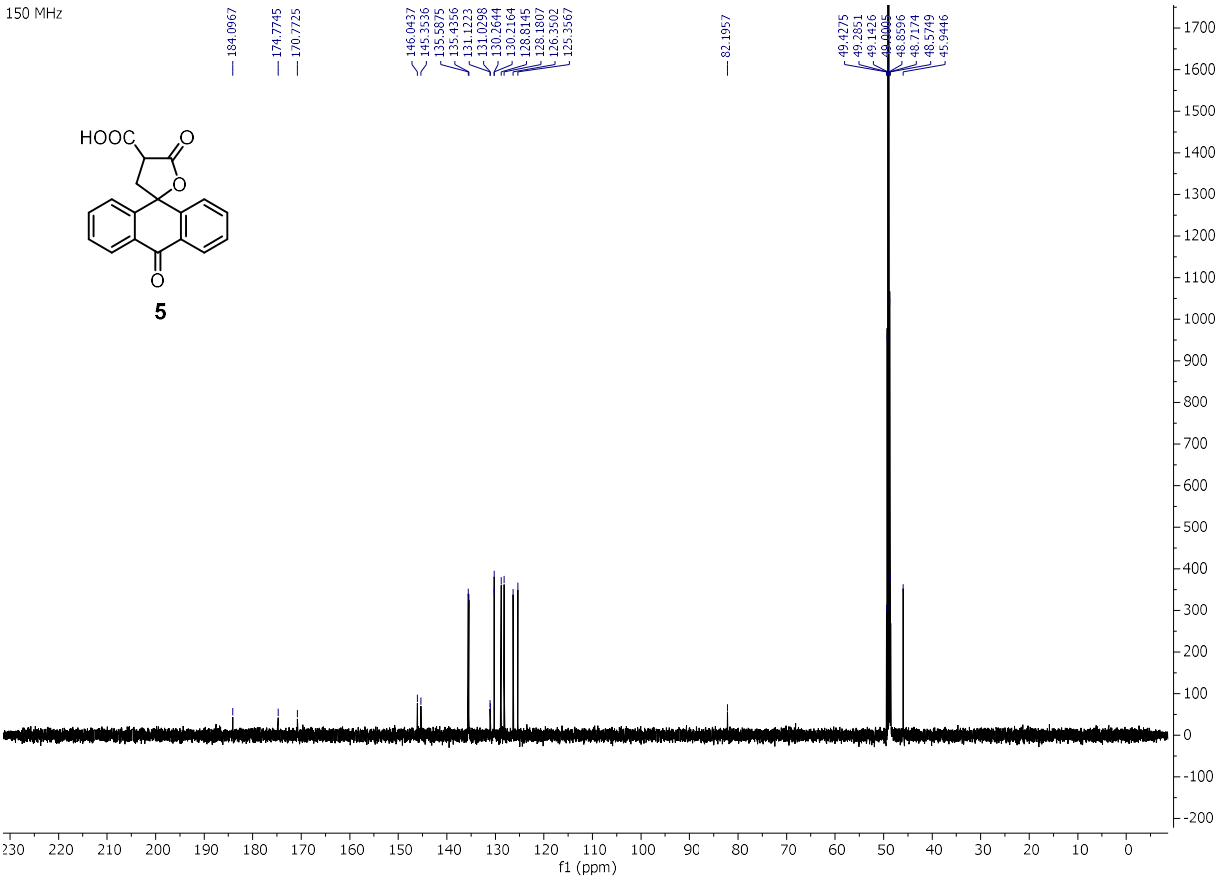

Figure S34. ^{13}C NMR spectrum of **5** in methanol-d_4

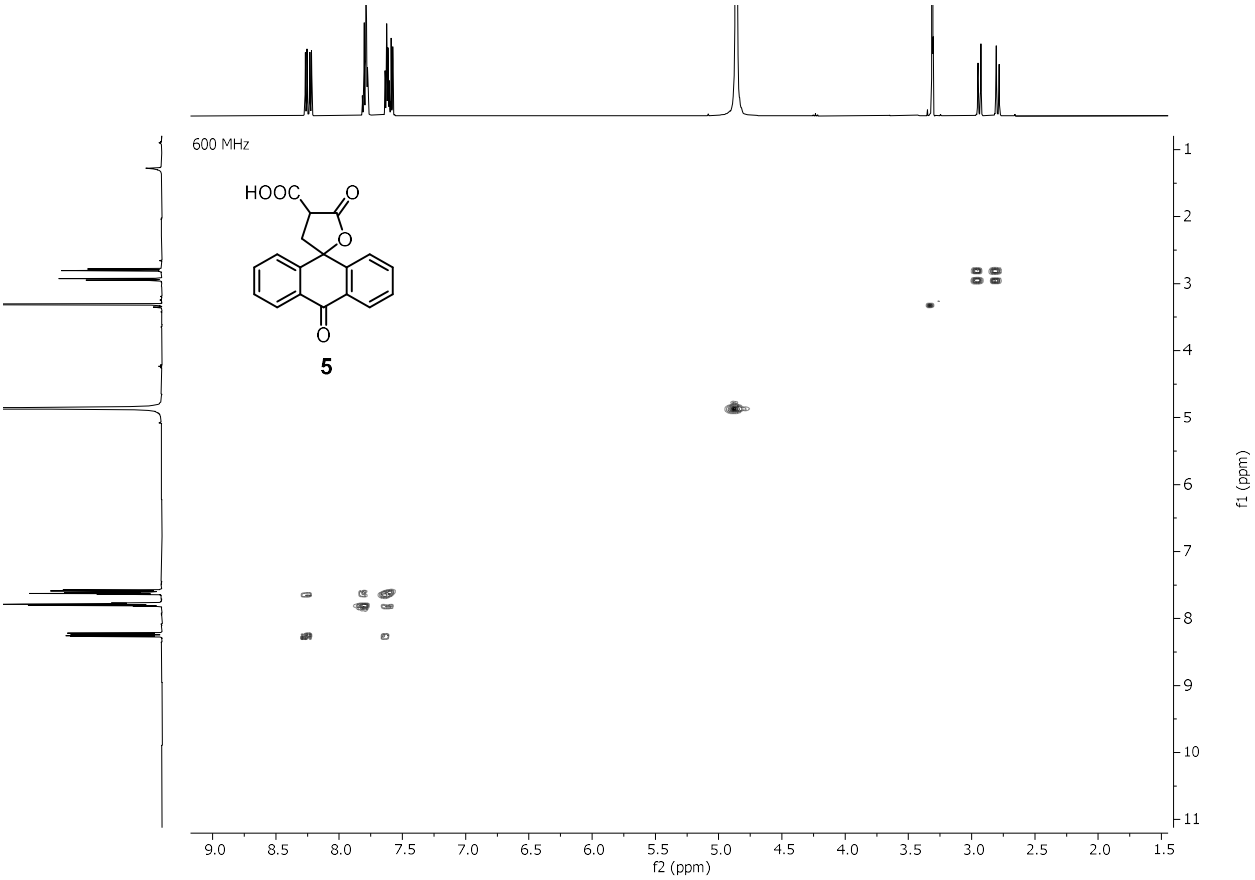

Figure S35. $^{1}H - {}^{1}H$ COSY spectrum of **5** in methanol-d_4

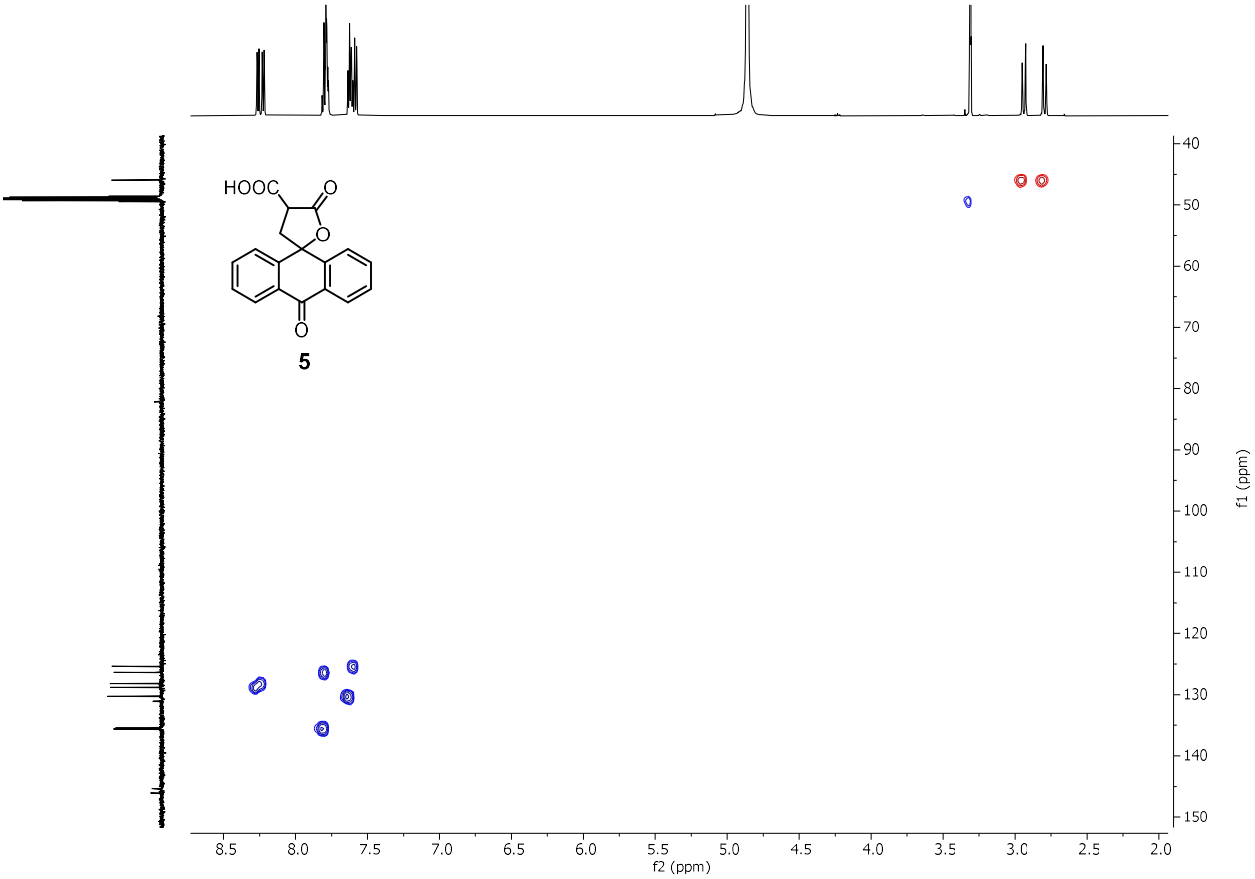

Figure S36. ^{1}H – ^{13}C HSQC spectrum of **5** in methanol-d_4

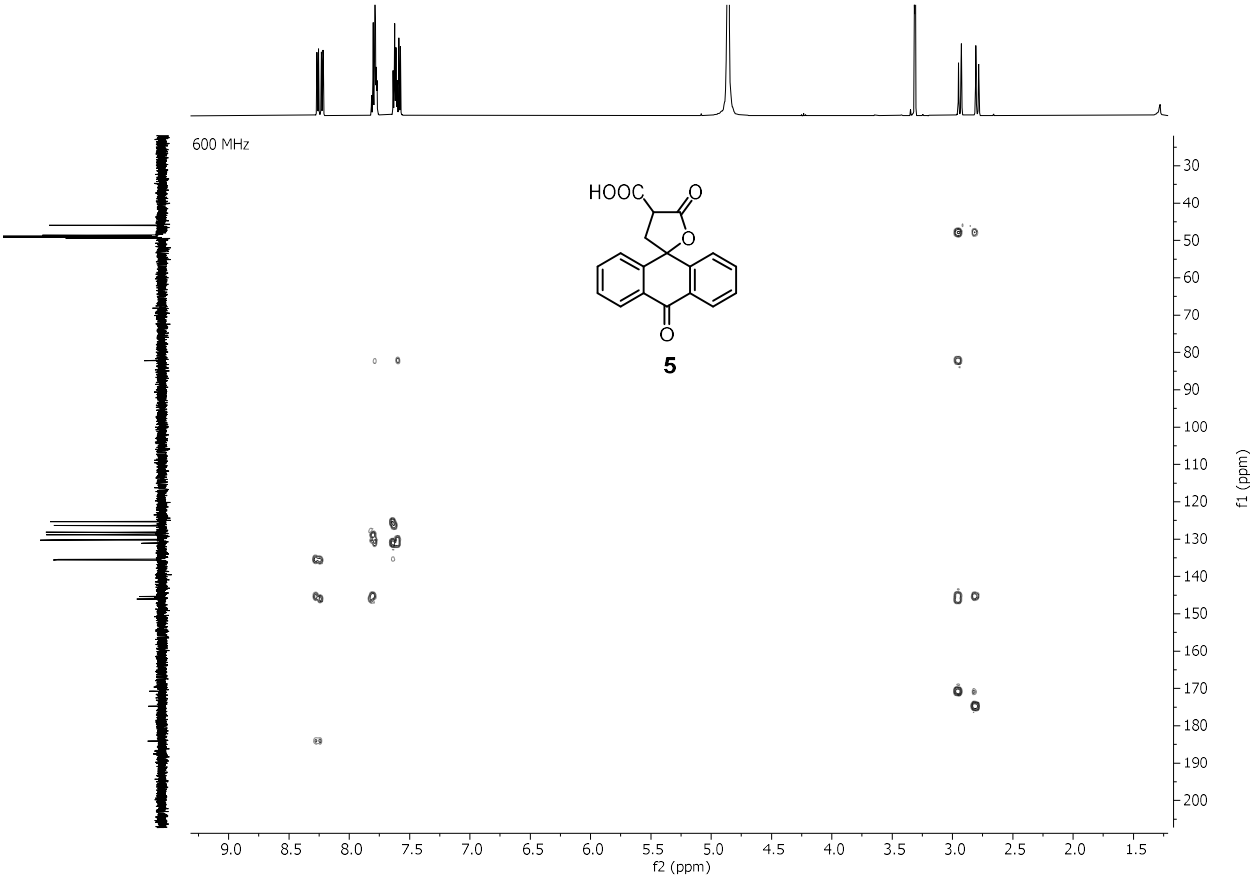

Figure S37. ^{1}H – ^{13}C HMBC spectrum of **5** in methanol-d_4

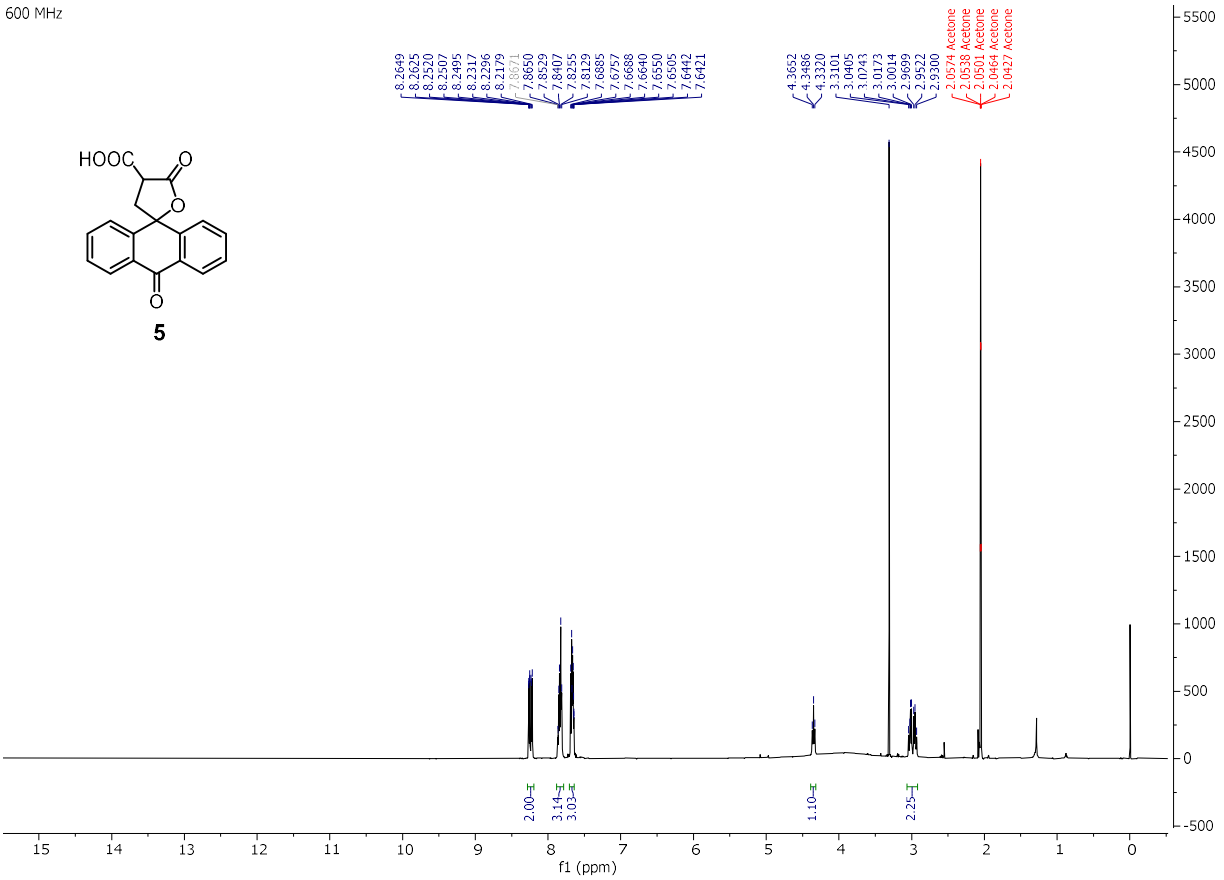

Figure S38. ^{1}H NMR spectrum of **5** in acetone-d_6

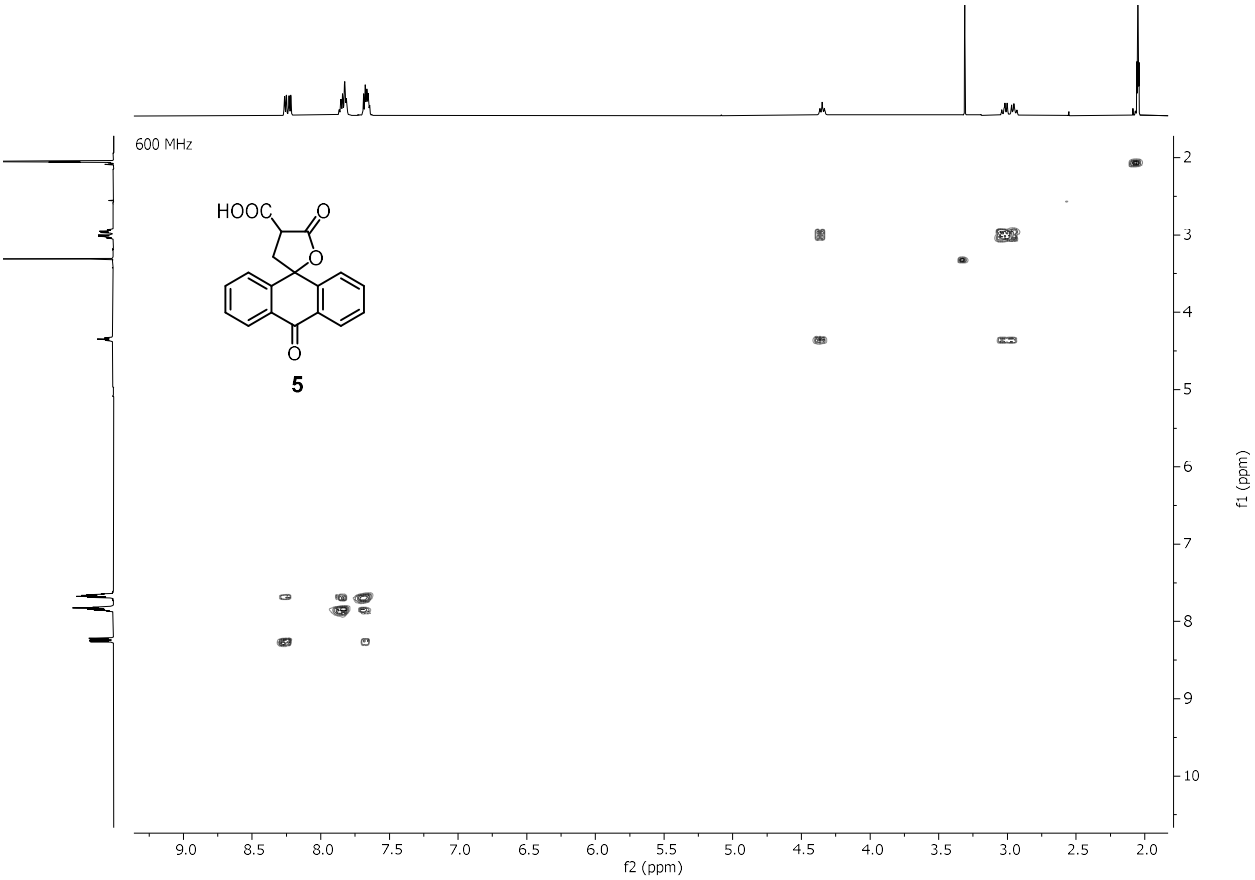

Figure S39. $^{1}H - {}^{1}H$ COSY spectrum of **5** in acetone-d_6

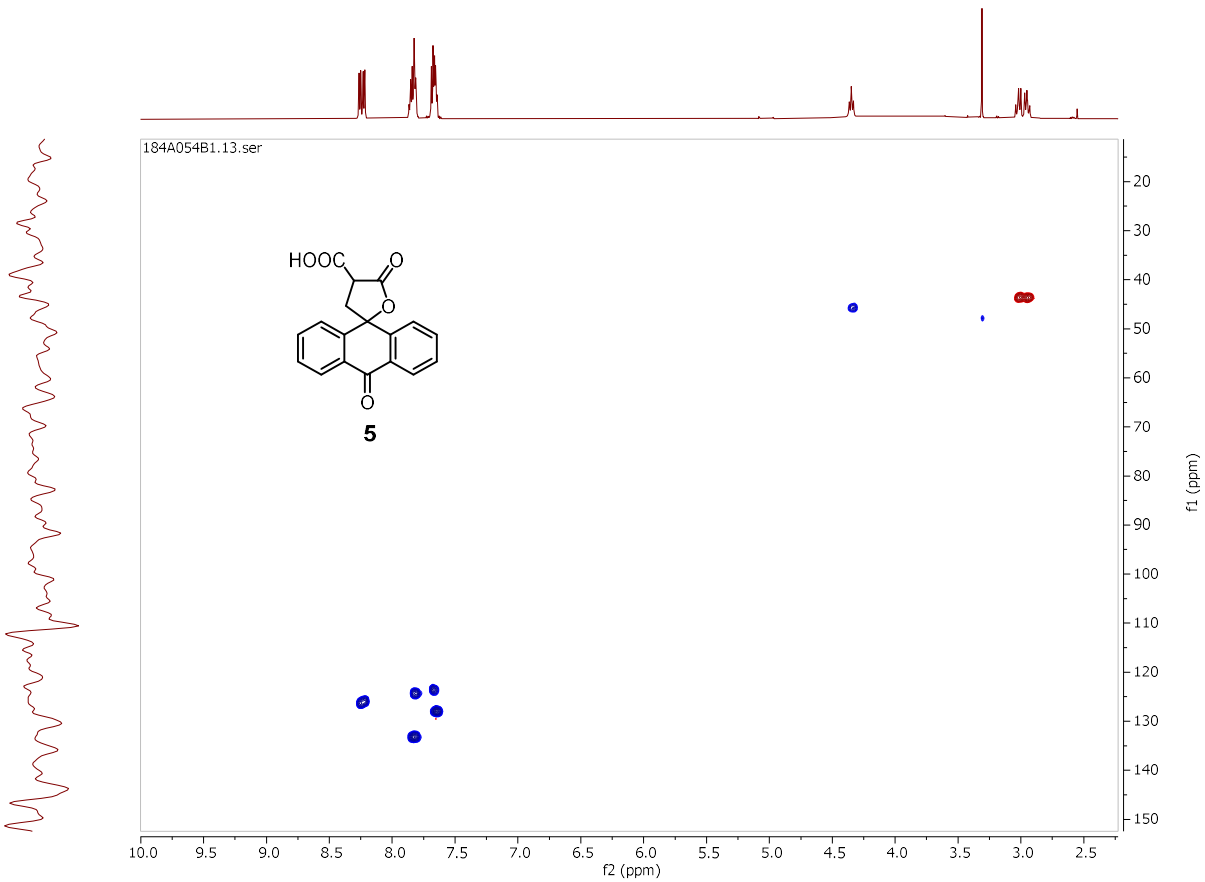

Figure S40. ^{1}H – ^{13}C NMR spectrum of **5** in acetone-d_6

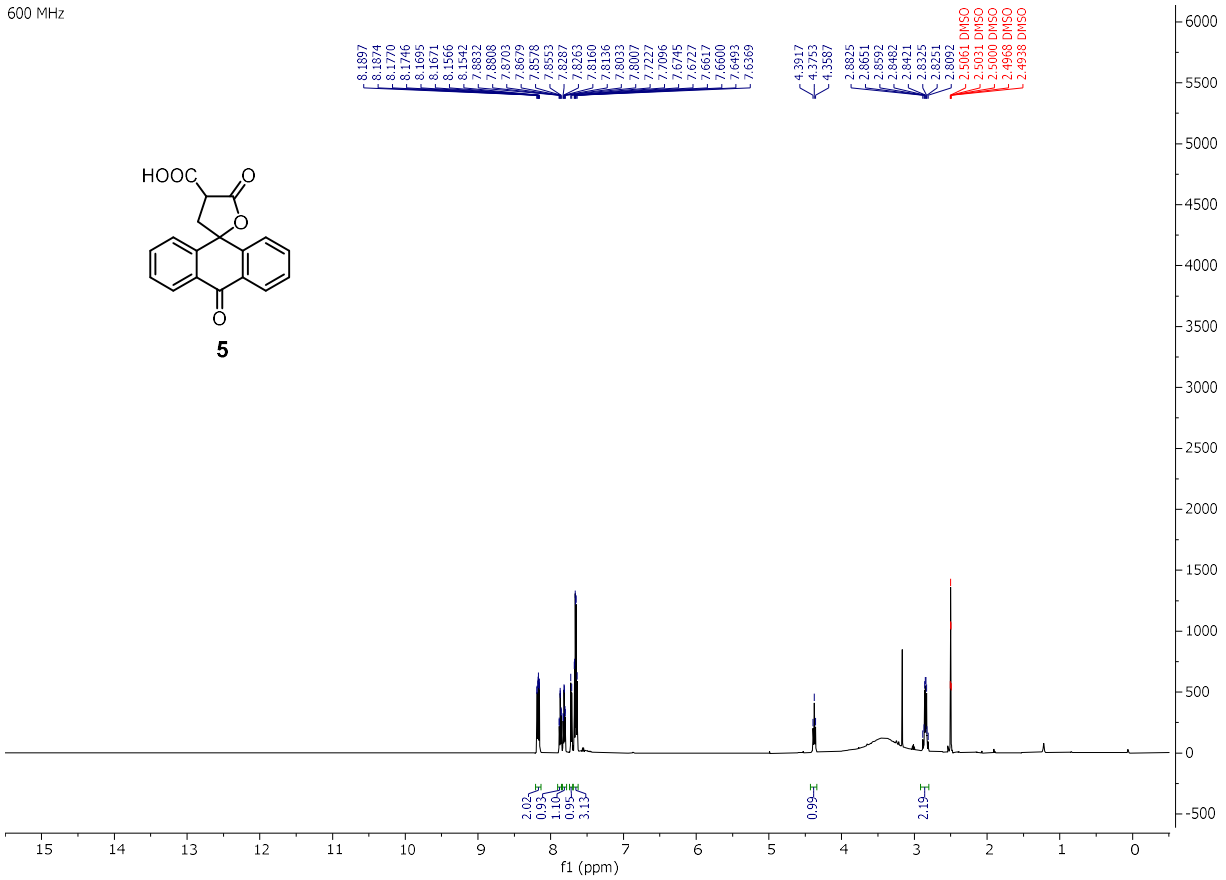

Figure S41. ^{1}H NMR spectrum of **5** in DMSO-d_6

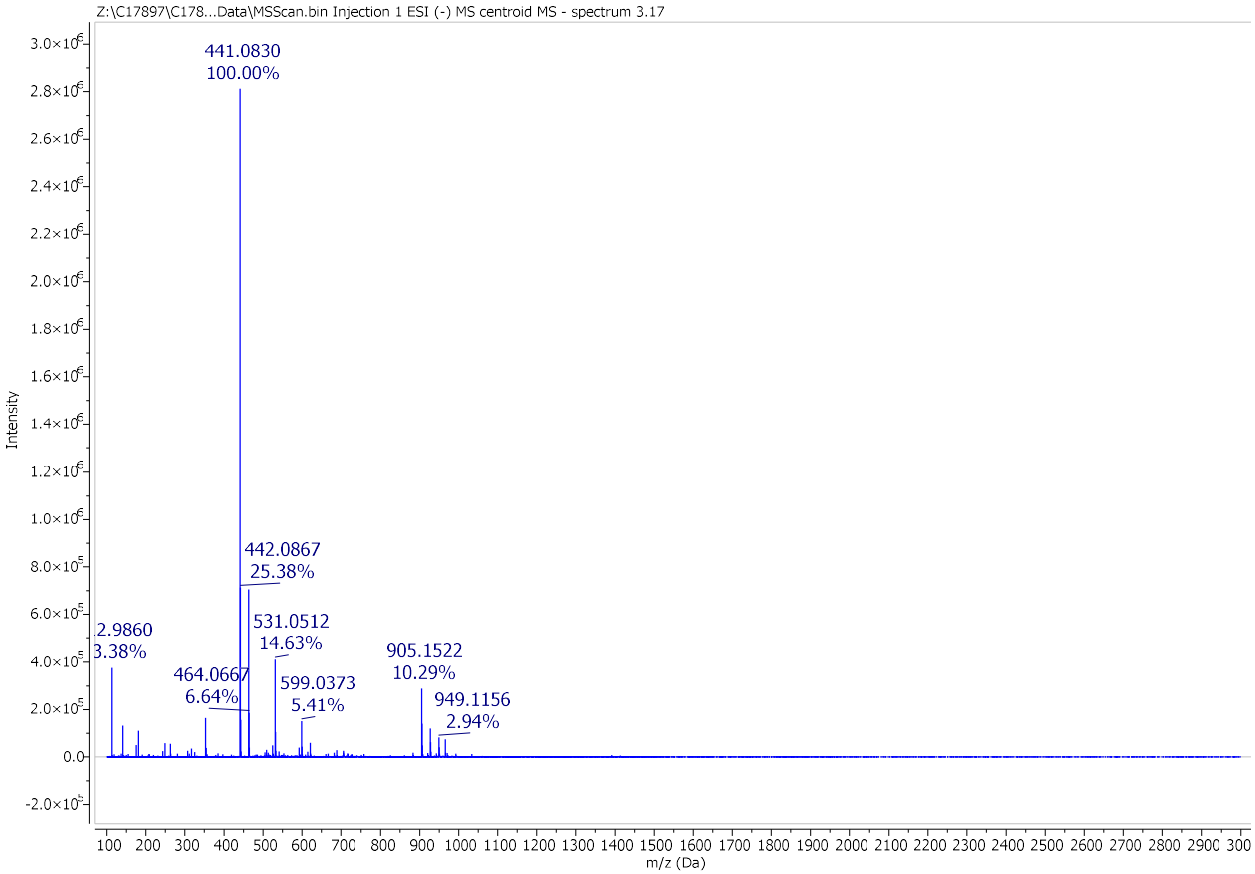

Figure S42. HRESIMS^{-} spectrum of **4**

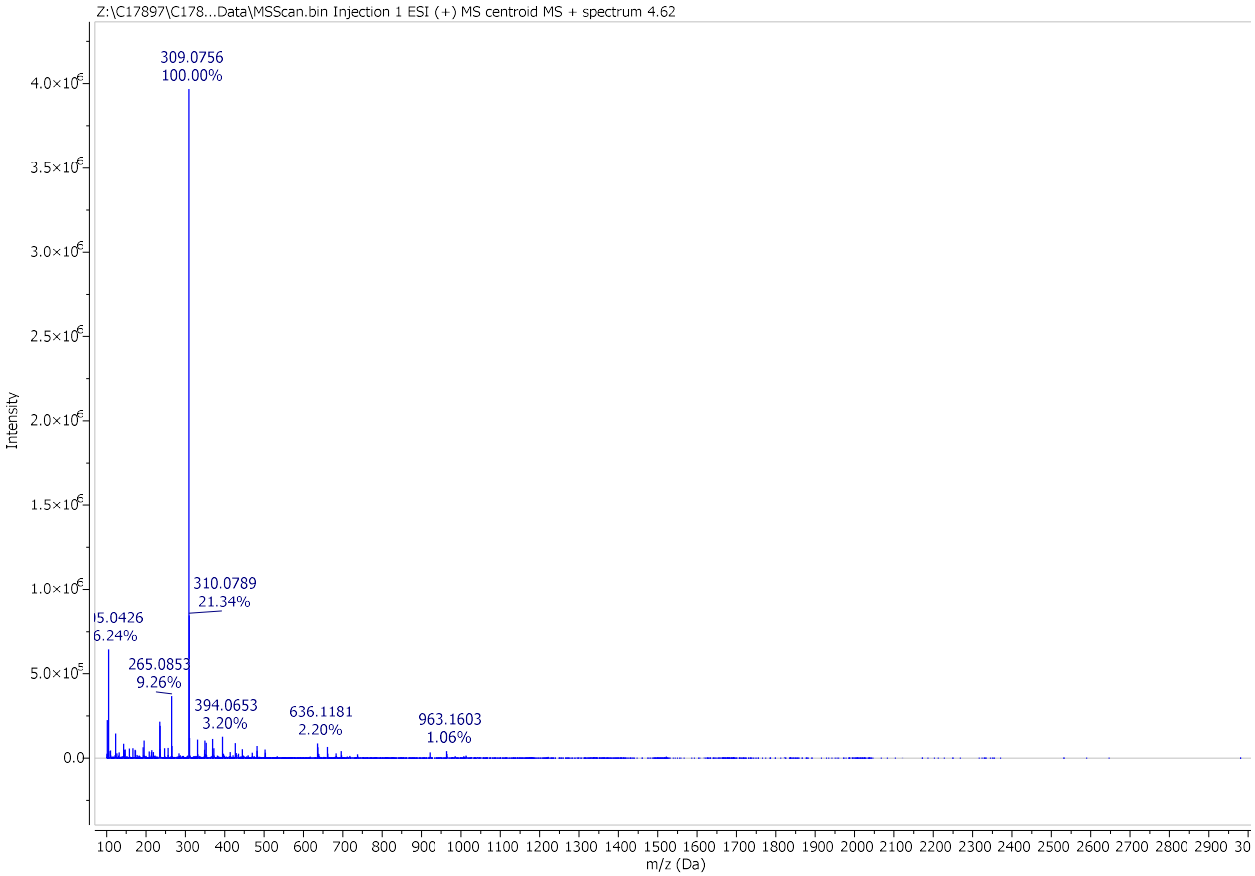

Figure S43. HRESIMS^{+} spectrum of **5**